Physikalisch-Technische Bundesanstalt
Braunschweig und Berlin

Report on

Key Comparison EURAMET.L-K3.2009

(Project # 1074)

Angle Comparison Using an Autocollimator

Final Report

Ralf D. Geckeler (PTB), Andreas Just (PTB),

Valentin Vasilev (BIM), Emilio Prieto (CEM), František Dvorácek (CMI),
Slobodan Zelenika (DMDM), Joanna Przybylska (GUM), Alexandru Duta (INM),
Ilya Victorov (INPL), Marco Pisani (INRIM), Fernanda Saraiva (IPQ),
Jose Antonio Salgado (LNE), Sitian Gao (NIM), Tonmueanwai Anusorn (NIMT),
Siew Leng Tan (NMC-A*STAR), Peter Cox (NMIA), Tsukasa Watanabe (NMIJ)
Andrew Lewis (NPL), K.P. Chaudhary (NPLI), Ruedi Thalmann (METAS),
Edit Banreti (MKEH), Alfiyati Nurul (RCM-LIPI), Roman Fira (SMU),
Tanfer Yandayan (TUBITAK-UME), Konstantin Chekirda (VNIIM),
Rob Bergmans (VSL), Antti Lassila (VTT)

Braunschweig, January 2018

Contents

1 Introduction

Autocollimators are versatile optical devices for the precise and contactless measurement of angles of reflecting surfaces. They are well suited for a broad range of applications in metrology and industrial manufacturing, e.g., angle adjustment, measurement of straightness, parallelism and rectangularity of machine tools, etc. In recent years, electronic autocollimators have also proved to be capable of providing highly accurate angle metrology for the form measurement of challenging optical surfaces. The importance of measurand traceability (via calibration) for this broad range of autocollimator applications supports the motivation for this comparison of the calibration capabilities of National Metrology Institutes (NMI).

As described in the Mutual Recognition Arrangement (MRA)[1], the metrological equivalence of national measurement standards will be determined by a set of comparisons chosen and organised by the Consultative Committees of the Comité International des Poids et Mesures (CIPM) working closely with the Regional Metrology Organisations (RMO). At the 13th meeting of the Working Group for Dimensional Metrology (WGDM), 24-25th September 2008, INRIM, Torino, Italy, and at the European Association of National Metrology Institutes (EURAMET) Technical Committee of Length (TC-L) Meeting, 6-7th October 2008, MIKES, Espoo, Finland, the Physikalisch-Technische Bundesanstalt (PTB) first proposed a comparison on the calibration of autocollimators. The initial proposal has been refined over the course of subsequent WGDM and EURAMET TC-L meetings and a total of 28 National Metrology Institutes (NMI) have agreed to join this Key Comparison (KC) as participants with the PTB acting as the pilot laboratory. In the end, a total of 26 NMIs followed through.

The KC was registered as EURAMET.L-K3.2009 'Angle comparison using an autocollimator' (Project # 1074) with the BIPM data base. After an extensive characterisation of the standard by PTB and the creation of a Technical Protocol (TP), data acquisition started in December 2009. Due to the large number of international participants, it ended in April 2016, covering a time span of more than six years.

As it represents the first such comparison which utilised an autocollimator as a standard, it provided opportunities for increasing our knowledge on these devices. This includes a substantial – though previously neglected – error source in precision metrology with autocollimators, specifically, changes in the air's refractive index, with a focus on the dominant impact of pressure changes. Pressure decreases with increasing elevation above sea level and is subject to substantial variation due to weather changes. It causes pressure-dependent changes in the autocollimator's angle response which are proportional to the measured angle and which increase linearly with the beam length between the autocollimator and the reflecting mirror. For the analysis of the data of this KC, PTB as the pilot laboratory had to characterise this effect in detail by use of extended theoretical and experimental investigations and derive strategies for accounting for the uncertainty contribution of this environmental influence. Additionally, the standard was damaged – and subsequently repaired – during transport early in the comparison. This necessitated the splitting of the comparison and the treatment of the autocollimator before and after repair as two separate standards. Due to these complexities, data analysis required longer than expected.

[1] The MRA was signed at the 21st General Conference of Weights and Measures on the 14th October 1999 in Paris; see information on the BIPM website (http://www.bipm.fr).

2 The standard

2.1 General requirements

The standard for this comparison, see Section 2.2, was chosen for the following reasons:

1. The comprehensive experience at the PTB in its calibration and the characterization of the parameters influencing the standard's angle response, see [2-1 – 2-5].
2. Its stability as demonstrated by repeated calibrations of individual instruments over several years at the PTB.
3. Its widespread use for precision angle metrology in research and industry.
4. Its commercial availability so that each participating laboratory may obtain, if desired, a standard of the same type.

2.2 Description of the standard

For this comparison, an electronic autocollimator type Elcomat 3000 by Möller-Wedel Optical GmbH (MWO), Wedel, Germany, see Figure 2-1, has been kindly made available by the manufacturer[2].

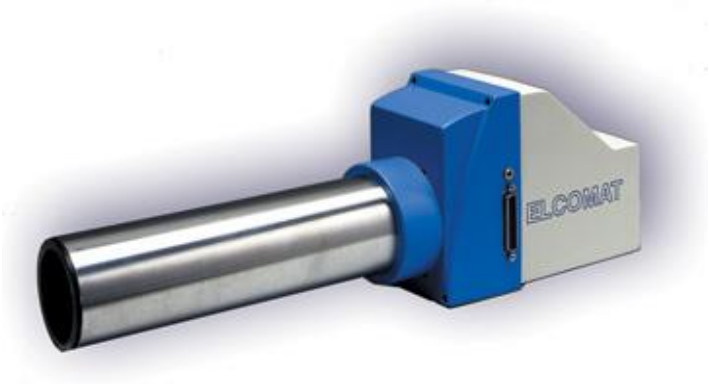

Figure 2-1. Elcomat 3000 autocollimator by Möller-Wedel Optical GmbH (MWO), Wedel, Germany (Figure courtesy MWO).

As all participants have been provided with a detailed technical manual of the autocollimator, so only its basic properties are summarised here shortly:

- Two axis electronic autocollimator (the comparison will be performed on the horizontal x-axis only)
- Measuring range: 2000 x 2000 arcsec (up to 2.5 m distance to the reflector)
- Highest resolution: 0.001 arcsec
- Focal length: 300 mm
- Diameter of the illuminated (effective) aperture: 32 mm (tube diameter: 65 mm)
- Dimensions: 420 x 95 x 135 mm
- Weight: 3.8 kg
- Serial number S.N. 900

[2] https://www.haag-streit.com/de/moeller-wedel-optical/

2.3 Mounting

An adjustable holder for the autocollimator with a double-sided clam fixture (type D65, MWO no. 223 024) was provided by the PTB (kindly made available by MWO). It allows the rotation of the autocollimator in its mount (around the autocollimator's optical axis) by 90° for the flexible measurement of the x-axis in a vertical orientation. As the autocollimator's angle deviations are stable with respect to rotations of its body, NMIs can calibrate the x-axis of the device in a horizontal or vertical orientation, depending on the requirements set by their equipment, and can avoid the use of additional optics for the rotation of the beam deflection plane.

2.4 References

[2-1] Just A, Krause M, Probst R, and Wittekopf R 2003 Calibration of high-resolution electronic autocollimators against an angle comparator *Metrologia* **40** 288-294

[2-2] Geckeler RD, Just A, Krause M, and Yashchuk VV 2010 Autocollimators for deflectometry: Current status and future progress *Nuclear Instruments and Methods in Physics Research Section A* **616** 140-146

[2-3] Geckeler RD and Just A 2008 Distance dependent influences on angle metrology with autocollimators in deflectometry *Proc. SPIE* **7077** 70770B 1-12

[2-4] Geckeler RD and Just A 2007 Optimized use and calibration of autocollimators in deflectometry *Proc. SPIE* **6704** 670407 1-12

[2-5] Geckeler RD, Artemiev NA, Barber SK, Just A, Lacey I, Kranz O, Smith BV, and Yashchuk VV 2016 Aperture alignment in autocollimator-based deflectometric profilometers *Rev. Sci. Instrum.* **87** 051906 1-8

3 Organisation

Following the guidelines set up by the Bureau International des Poids et Mesures (BIPM)[3], the PTB drafted a TP after having solicited responses to a preliminary description of the comparison by several members from a provisional list of NMIs. Their technical comments have been included in all drafts of the TP and of the analysis of the data. This RMO Key Comparison EURAMET.L-K3.2009 (EURAMET project #1074) has been operated to support the MRA of the CIPM and its progress and results have been reported regularly to EURAMET TC-L as well as the WG-MRA of the CCL. By their declared intention to participate in this comparison, the laboratories did accept the general instructions, those in the TP, and committed themselves to follow the procedures.

3.1 Requirements for participation

Per WGDM recommendation No.2 (document CCDM/WGDM/97-50b), the participating laboratories should offer this measurement as a calibration service (now or in future), be willing to participate in a regional comparison to provide a link between the interregional and the regional comparisons and have a measurement uncertainty below a certain level. This level shall be fixed to approximately 1 arcsec standard uncertainty. (However, most of the participants do offer calibrations with substantially smaller measurement uncertainties.)

Different metrological regions are represented in this comparison with a focus on NMIs from the EURAMET and from the Asia Pacific Metrology Programme (APMP). Calls for participation were issued at several WGDM and EURAMET TC-L meeting from September 2008 on and include everybody who was willing to participate in the autocollimator comparison.

3.2 Participants

The following Table 3-1 provides the final list of the participants.

Table 3-1. List of participants.

Institute	Adress	Contact
A-STAR	1 Science Park Drive Singapore 118221 Singapore	Siew Leng Tan Phone: +65 6279 1938 Fax: +65 6279 1994 tan_siew_leng@nmc.a-star.edu.sg
BIM	Bulgarian Institute of Metrology GD National Center of Metrology 52B, G.M. Dimitrov Blvd 1040 Sofia Bulgaria	Valentin Vasilev Phone: + 359 2 970 2719 Fax: + 359 2 970 2735 v.vasilev@bim.government.bg
CEM	CENTRO ESPAÑOL DE METROLOGÍA Alfar, 2 Tres Cantos - 28760 Madrid Spain	Emilio Prieto Phone: +34 918074716 Fax: +34 918074807 eprieto@cem.minetur.es
CMI	CMI OI Liberec	Dvorácek František

[3] http://www.bipm.fr

	Slunecná 23 460 01 Liberec Czech Republic	Phone: +420 485 107 532 Fax: +420 485 104 466 fdvoracek@cmi.cz pkren@cmi.cz pballing@cmi.cz
DMDM	Directorate of Measures and Precious Metals Mike Alasa 14 11000 Belgrade Serbia	Zelenika Slobodan Phone: +381 112024 421 Fax: +381 112181 668 zelenika@dmdm.rs
GUM	Central Office of Measures (GUM) Head of Angle Laboratory ul. Elektoralna 2 00-139 Warszawa Poland	Przybylska Joanna Phone: +48 22 581 95 58 Fax: +48 22 581 93 92 j.przybylska@gum.gov.pl
INM	INM Bucharest Sos. Vitan-Barzesti 11 Sector 4 042122 Bucharest Romania	Duta Alexandru Phone: 004021 334 50 60 Fax: 004021 334 53 45 alexandru.duta@inm.ro luciangrozea@gmail.com
INPL	Head Physical Standards Division National Physical Laboratory of Israel Givar Ram Danciger A Bldg 91904 Jerusalem Israel	Victorov Ilya Phone: +972 2 6303508 Fax: +972 2 6303516 ilya.victorov@economy.gov.il
INRIM	INRIM Strada delle Cacce, 73 10135 Torino Italy	Pisani Marco Astrua Milena Fax: +39 011 3919 959 m.pisani@inrim.it m.astrua@inrim.it
IPQ	Instituto Português da Qualidade Área de Comprimento, Tempo e Fotometria Rua António Gião, 2, 2829-513 CAPARICA Portugal	Saraiva Fernanda Phone: +351 21 2948160 or +351 21 2948156 Fax: +351 21 2948188 fsaraiva@ipq.pt
RCM-LIPI	Pusat Penelitian Metrologi-LIPI Komplek Puspiptek, Ged. 420, Setu,Tangerang Selatan, Banten, 15314 Indonesia	Nurul Alfiyati Phone: +62 21 7560562 ext 3078 Fax: +62 21 7560568 nurul.alfi@gmail.com nurul.alfi@kim.lipi.go.id probo@kim.lipi.go.id
LNE	Head of Dimensional Metrology Department Mechanical Metrology Division DMSI Laboratoire national de métrologie et d'essais 1, Rue Gaston Boissier 75724 Paris Cedex 15 France	Salgado Jose-Antonio Phone: +33 1 40 43 39 57 Jose.Salgado@lne.fr

METAS	Federal Institute of Metrology METAS Lindenweg 50 CH-3003 Bern-Wabern Switzerland	Thalmann Ruedi Phone: +41 31 58 387 038 Fax: +41 31 58 387 021 Rudolf.Thalmann@metas.ch
MIKES (VTT)	Group manager, Length Centre for Metrology and Accreditation P.O. box 9 (Tekniikantie 1) FIN-02151 Espoo Finnland	Lassila Antti Hemming Björn Phone: +358 10 6054 413 GSM: +358 40 7678584 Fax: +358 10 6054 499 Antti.Lassila@vtt.fi Bjorn.Hemming@vtt.fi
MKEH	Metrology Division Department of Mechanical Measurements Nemetvolgyi ut 37-39 Budapest 1124 HUNGARY	Banreti Edit Phone: +361 4585 997 Fax: +361 4585 927 banretie@mkeh.hu
NIM	National Institute of Metrology Length Division No 18 Bei San Huan Dong Lu Beijing, 100013 China	Gao Sitian Phone: +86 10 6452 4903 Fax: +86 10 6421 8703 gaost@nim.ac.cn
NMIA	National Measurement Institute 1/153 Bertie Street Port Melbourne VIC 3207 Australia	Cox Peter Phone: +61 3 9644 4906 Fax: +61 3 9644 4900 peter.cox@measurement.gov.au
NMIJ	National Metrology Inst. of Japan (NMIJ) Dimensional Standards Section AIST Tsukuba Central 3 1-1-1 Umezono, Tsukuba, Ibaraki 305-8563 Japan	Watanabe Tsukasa Fujimoto Hiroyuki Phone +81 29 861 40 41 or 42 91 Fax: +81 29 861 4042 t.watanabe@aist.go.jp h.fujimoto@aist.go.jp
NIMT	Department of Dimensional Metrology National Institute of Metrology Thailand 3/5 Moo 3, Klong 5, Klong Luang Pathumthani 12120 Thailand	Anusorn Tonmueanwai Phone: +662 5775100 Fax: +662 5775088 anusorn@nimt.or.th
NPL	NPL Room F5-A4 Engineering Measurement Division United Kingdom	Lewis Andrew Flack David Phone: +44 208 943 6074 Fax: +44 208 614 0533 Andrew.Lewis@npl.co.uk David.Flack@npl.co.uk
NPLI	LENGTH & DIMENSION STANDARDS National Physical Laboratory, Dr. K.S. Krishnan Road, New Delhi - 110012,	Chaudhary K.P. Phone: +91 11 25732865 Fax: +91 11 25726938 kpc@mail.nplindia.ernet.in

	India	
PTB	Physikalisch-Technische Bundesanstalt 5.23 Angle Metrology Bundesallee 100 D - 38116 Braunschweig Germany	Geckeler Ralf D. Just Andreas Phone: +49 531 592 5220 Fax: +49 531 592 69 5220 ralf.geckeler@ptb.de andreas.just@ptb.de
SMU	Slovenský Metrologický ústav Karloveská 63 842 55 Bratislava Slovak Republic	Fira Roman Phone: +421 2 60294232 fira@smu.gov.sk
UME	TUBITAK-UME Anibal Cad. Gebze Yerleşkesi PK54 - 41470 Gebze-Kocaeli Turkey	Yandayan Tanfer Phone: +90 262 679 5000 (ext. 5300) Fax: +90 262 679 5001 tanfer.yandayan@tubitak.gov.tr okan.ganioglu@tubitak.gov.tr asli.akgoz@tubitak.gov.tr
VNIIM	St. Petersburg 190005 Moskovsky pr., 19 Russia	Chekirda Konstantin Phone: +7 812 323-96-80 Fax: +7 812 323- 96-63 K.V.Chekirda@vniim.ru
VSL	Thijsseweg 11 2629 JA Delft Netherlands	Bergmans Rob Phone: +31 15 2691500 Fax: +31 15 2691641 rbergmans@vsl.nl rkoops@vsl.nl

3.3 Time schedule

The comparison had been carried out in a mixed form, circulation and star-type. After the standard had been circulated in a region, it was sent back to the pilot laboratory, PTB, for recalibration (stability / quality inspection) before circulation within the next region.

Table 3-2. Time schedule of the comparison.

Loop 1: Measurement uncertainty *U* (k=2) < 0.1 arcsec (with exceptions)

Germany	PTB (pilot)	12 / 2009
United Kingdom	NPL	01 / 2010
Netherlands	VSL	02 / 2010
Finland	MIKES (now VTT)	03 / 2010
Switzerland	METAS	04 / 2010
Germany	PTB (pilot)	05 / 2010
Italy	INRIM	06 / 2010
Turkey	UME	07 / 2010
Romania	INM	08 / 2010
France	LNE	09 / 2010
Germany	PTB (pilot)	11 / 2010

Loop 2: Measurement uncertainty *U* (k=2) ≥ 0.1 arcsec

Germany	PTB (pilot)	04 / 2011
Hungary	MKEH	05 / 2011
Israel	INPL	07 / 2011
Czech Republic	CMI	09 / 2011
Poland	GUM	11 / 2011
Slovak Republic	SMU	12 / 2011
Germany	PTB (pilot)	02 / 2012
Spain	CEM	03 / 2012
Greece	EIM	04 / 2012
Belgium	SMD	05 / 2012
Netherlands	VSL	07 / 2012
Portugal	IPQ	09 / 2012
Italy	INRIM	11 / 2012
Germany	PTB (pilot)	12 / 2012

Loop 3: APMP Asian-pacific participants (part 1)

Germany	PTB (pilot)	12 / 2012
Japan	NMIJ	02 / 2013
Australia	NMIA	04 / 2013
China	NIM	08 / 2013
India	NPLI	10 / 2013
Germany	PTB (pilot)	02 / 2014

Loop 4: APMP Asian-pacific participants (part 2) and new European participants

Germany	PTB (pilot)	02 / 2014
Singapore	A-STAR	06 / 2014
Thailand	NIMT	07 / 2014
Serbia	DMDM	09 / 2014
Germany	PTB (pilot)	10 / 2014
Indonesia	RCM-LIPI	11 / 2014
Germany	PTB (pilot)	04 / 2015
Bulgaria	BIM	05 / 2015
Slovak Republic	SMU	07 / 2015
Russia	VNIIM	09 / 2015
Germany	PTB (pilot)	11 / 2015
Czech Republic	CMI	01 / 2016
Germany	PTB (pilot)	04 / 2016

In Section 8, we have provided the comments on their measurements submitted by the participants during this KC. We present an abbreviated list here, together with additional comments from PTB:

- Due to the instable political situation, the pilot laboratory decided to exclude NSCL (Syria) from the list of participants (letter from 2013-12-04).
- SCL (Hong Kong) has decided not to take part in this comparison immediately before its start.
- SMD (Belgium) and EIM (Greece) have withdrawn their participation after performing their measurements.
- VSL (Netherlands), INRIM (Italy), SMU (Slovak Republic), and CMI (Czech Republic) requested to carry out repeat calibration.
- VSL and SMU reported damages to their calibration devices.
- Participants who had measured the standard between the occurrence of the transport damage and its discovery by PTB's monitoring measurements were offered the opportunity to repeat their measurements after the repair of the standard, see Section 7.2 for details. INRIM (Italy) accepted the offer.
- CMI developed a novel calibration set-up during the comparison. The measurements with the old and new set-up were included in this comparison. However, the measurements performed with the novel set-up were not included in the KCRV.

4 Measuring instructions

There are several factors influencing the angle response / calibration of an autocollimator which can be categorised as external vs. internal. Internal factors are specific to the individual autocollimator with its internal design (and are therefore generally beyond user control). External factors are given by the measuring conditions under which the device is used (and can thus be specified by the user).

Based on our comprehensive experience in autocollimator calibration at the PTB, the latter group of factors includes the following parameters (see [2-2 – 2-5] for details):

- Reflectivity of the mirror
- Curvature of the mirror
- Distance (optical path length) between the autocollimator and the mirror
- If an aperture stop is used:
    - Diameter and shape of the aperture stop
    - Position of the aperture stop along the autocollimator's optical axis
    - Lateral position of the aperture stop perpendicular to the optical axis

According to our experience in autocollimator calibration, significant differences in the calibration may occur in case of changes in one or several parameters.

With the measuring instructions presented in the TP, we attempted to achieve a balance between allowing NMIs to calibrate the reference autocollimator under measurement conditions which are typical for routine calibrations at their facilities, and ensuring optimal comparability of the calibration results achieved at different NMIs. On the one hand, calibration results should provide realistic information on the calibration capabilities and limits at each NMI, on the other hand, systematic errors due to changes in the measuring conditions must be avoided, as they may not be accounted for by the stated measurement uncertainties.

In case of deviations of the measuring conditions from the stated specifications, e.g., due to constraints of the calibration set-up at the NMI, a detailed documentation of the changed condition(s) was provided by the participants.

4.1 Plane mirror

Each participating NMI could use its own plane mirror which is normally used for calibrations for customers. To avoid systematic errors due to the mirror's curvature and reflectivity, we specified the following parameters:

- Reflectivity: Use of a mirror with a metallic coating (usually aluminium) to obtain a reflectivity approaching 100%.
- Size of the reflecting area: 50 mm in diameter to provide an unobstructed reflection over the effective, illuminated autocollimator aperture (32 mm in diameter).
- Flatness deviation of the measurement face: $\lambda/8$ (peak-to-valley) for a region at least 32 mm in diameter.

As deviations from the stated measuring conditions may alter the autocollimator's angle response significantly [2-1 – 2-5], we considered the realization of these parameters as essential. If available, participants provided optional documentation on their mirrors (flatness deviation, reflectivity).

In addition, each participating NMI could perform additional calibrations with a precision plane mirror (Ref. No. 280 345; S.N. 150) provided by the PTB to ensure optimal comparability of the results (optional), see Figure 4-1. In that case, it was recommended to use face 1 of the double-sided mirror.

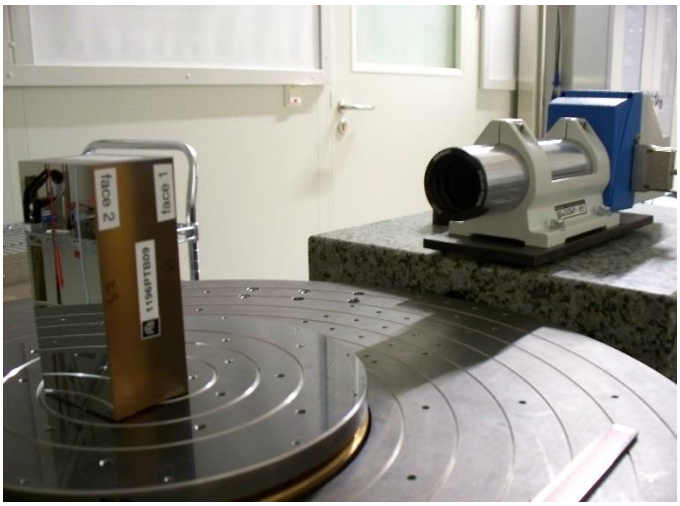

Figure 4-1. Precision plane mirror provided by the PTB (its use was optional).

We have investigated the influence of flatness deviations of the reflecting mirror on the angle response of autocollimators. In the case of two mirrors with different flatness deviations of 4 nm and 20 nm (root-mean-square), systematic changes in the angle response of a few 0.01 arcsec were found [2-2].

4.2 Distance autocollimator - mirror

In the case of different distances between the autocollimator and the reflecting mirror, the beam returning to the autocollimator follows different paths through its optics. In conjunction with aberrations of the optical components and errors in their alignment (and that of the CCD detector), angle deviations are introduced which are varying as a function of the distance to the mirror [2-3].

Each participating NMI could choose the distance between the autocollimator and the reflecting face of the plane mirror according to their usual specifications for calibrations. They provided information on the distance from the front end of the autocollimator's tube (which contains the objective) to the reflecting surface in their measurement documentations.

However, where it was possible with their calibration set-up, we strongly recommended to use a distance of 300 mm (equal to the focal length of the autocollimator) as, in this case, error influences are minimised. Additionally, we have demonstrated significant changes in the angle response of autocollimators in the case of a variable distance to the reflecting mirror [2-3].

4.3 Autocollimator aperture

To avoid the vignetting of the autocollimator's measuring beam returning from the mirror [2-4] and issues regarding the positioning of a beam-limiting diaphragm [2-5], no diaphragm was used. Therefore, the full illuminated autocollimator aperture (32 mm in diameter) was used in this comparison.

4.4 Measurement ranges and steps

The measurement deviations of autocollimators cover a wide range of angular scales, extending from a few arcseconds (connected to the pixels of the autocollimator's CCD detector) to the full measurement range (due to aberrations in the autocollimator's optical elements and detector misalignment).

Therefore, to appropriately sample the angle deviations on both short and long angular scales, we recommended two different measurement ranges for the comparison:

- Measurement range 1: $\pm$ 1000 arcsec in steps of 10 arcsec
- Measurement range 2: $\pm$ 10 arcsec in steps of 0.1 arcsec

For the comparison, calibrations had to be performed on the x-axis of the autocollimator.

If possible, we asked the participants to perform their measurements at the specified values as indicated by the autocollimator, i.e., the angular positioning of the calibration system is guided by the autocollimator. It was recommended to set the starting position to zero to better than 0.1 arcsec.

Qualification #1: If calibrations were not possible over the entire angle range, participants were allowed to calibrate over a limited range.

Qualification #2: If calibrations could not be performed at all specified measurement points (e.g., due to manual operation of the equipment), participants were allowed to calibrate at a selected subset of points. In this case, we suggest choosing a step width which is a multiple of the recommended step width.

Qualification #3: There is a small subset of participants which were not able to perform the calibrations according to the given recommendations even when taking the qualifications into consideration, e.g., due to a fixed step width which is predetermined by their calibration equipment. In this case, calibrations could be performed as specified by the equipment. The pilot laboratory, PTB, did accommodate the measurements by means of an appropriate interpolation of the provided data to conform to the specified sampling points.

4.5 Adjustment procedures

Each participating NMI was asked to follow its own adjustment procedures for autocollimator calibration as specified in their manuals. In Figure 4-2, the measurement set-up for the calibration of electronic autocollimators against the primary angle reference of the PTB, the angle comparator WMT 220 [4-1 – 4-3], is presented. The optical axis and the measuring axes of the autocollimator, as well as the plane mirror, need to be adjusted with respect to the comparator's rotational axis and the associated rotation plane. As an example and a guideline, in Table 4-1, we provide a description of our own adjustment procedures at the PTB.

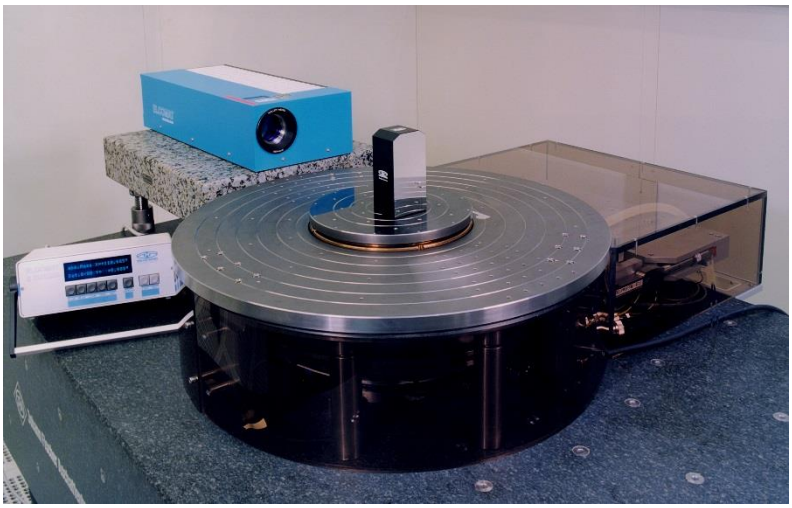

Figure 4-2. Set-up for the calibration of electronic autocollimators against the primary angle reference of PTB, the angle comparator WMT 220. The autocollimator and the plane mirror need to be adjusted relative to the comparator as described in the text.

Table 4-1. Adjustment procedures for autocollimator calibration at the PTB.

#	Adjustment step(s)	Tolerance
1	The height and lateral position of the autocollimator is adjusted with respect to the plane mirror so that the illuminated aperture of the autocollimator is entirely covered (to avoid vignetting). For the adjustment steps 1-2, the laser attachment[4], which is supplied with the autocollimator, can be used.	Mirror covers illuminated autocollimator aperture
2	The optical axis of the autocollimators is adjusted to intersect the rotational axis of the angle comparator.	<= 1 mm
3	The front surface of the plane mirror is adjusted with respect to the rotational axis of the angle comparator (so that the surface incorporates the axis).	<= 1 mm
4	The autocollimator's x measurement axis is adjusted parallel to the rotational plane of the angle comparator by rotating the autocollimator in its holder around its optical axis. When the comparator is rotated, the change Δx of the angle in the x-axis of $\pm$1000 arcsec must result in minimal change Δy in the y-axis reading.	$\Delta y / \Delta x$ < 0.001
5	The front surface of the plane mirror is adjusted to be orthogonal to the rotation plane of the angle comparator (done by reversal measurements at 0° and 180° rotational angle by use of a double-side mirror).	< 1 arcsec
6	The optical axis of the autocollimators is adjusted to be orthogonal to the front surface of the plane mirror (and therefore parallel to the rotational plane of the angle comparator). The autocollimator is adjusted until the y-axis reading is close to zero.	< 1 arcsec
7	The plane mirror is rotated by the angle comparator to the starting position so that the reading of the x-axis of the autocollimator is close to zero.	< 0.1 arcsec

[4] For instructions on the use of the laser attachment (MWO no. 219 717), see the Elcomat 3000 manual.

4.6 Autocollimator settings

For the measurements, participants were asked to consider the following autocollimator settings:

- Switch to 'abs' setting (E3000 Manual, p. 18).
- Set unit to 'arcsec' (E3000 Manual, p. 14).
- Resolution (E3000 Manual, p. 16): This setting affects the resolution of the display only; it does not affect the values which are provided by the computer interfaces.
- Protocol for the RS-232 computer interface (E3000 Manual, p. 17 and p. 19): We strongly recommend to use the 'text protocol', especially for participants with low measurement uncertainties, because the data transfer is more reliable and its resolution is higher (0.001 arcsec in comparison to 0.01 arcsec for the 'compatible' format). Please do not use the USB computer interface as we have not tested its reliability for this comparison.

4.7 References

[4-1] Probst R, Wittekopf R, Krause M, Dangschat H and Ernst A 1998 The new PTB angle comparator *Meas. Sci. Technol*. **9** 1059-1066

[4-2] Just A, Krause M, Probst R, Bosse H, Haunerdinger H, Spaeth C, Metz G and Israel W 2009 Comparison of angle standards with the aid of a high-resolution angle encoder *Precis. Eng.* **33(4)** 530-533

[4-3] Geckeler RD, Link A, Krause M, and Elster C 2014 Capabilities and limitations of the self-calibration of angle encoders *Meas. Sci. Technol.* **25** 055003 1-10

5 Environmental influences on the standard

Co-authored with Petr Křen, Czech Metrology Institute (CMI)

5.1 Introduction

In this section, we discuss a substantial – though previously neglected – error source in precision metrology with autocollimators, specifically, changes in the air's refractive index, with a focus on the dominant impact of pressure changes. Pressure decreases with increasing elevation above sea level and is subject to substantial variation due to weather changes. It causes changes in the autocollimator's angle response which are proportional to the mirror's tilt angle, i.e., pressure changes introduce a linear component to its measuring deviations. In a separate publication, we characterise this influence in detail by use of extended theoretical and experimental investigations and derive strategies for correcting it [5-1]. Here, we present an abbreviated treatment and focus on its implications for the comparison at hand.

5.2 Influence on autocollimator measurements

The central optical element of an autocollimator is its objective. It acts as a lever which translates the tilt angle of the beam returning from the reflecting surface into a shift of a reticle image on a detector which is roughly proportional to the tilt angle times the objective's focal length. A lens focuses light by utilising the light's refraction at specially shaped glass-air boundaries. Its focal length, therefore, depends not only on lens geometry, but also on the ratio of the refractive indices of its bulk material and that of the surrounding air. The refractive index of air depends on several influencing parameters, such as its temperature, pressure, and humidity, see the Edlén equation [5-2, 5-3]. Well controlled, air-conditioned laboratory environments typically usually feature highly stable temperatures as well as limited changes in humidity. Air pressure, in contrast, is usually not regulated. It decreases with increased elevation above sea level and is subject to substantial long- and short-term variations due to weather changes. It is by far the most dominating factor in these environments, as demonstrated by [5-2, 5-3].

We make use of an idealised autocollimator model, based on a thin-lens approximation of its objective [5-1]. For small tilt angles α of the reflector, with $\tan(2\alpha) \approx 2\alpha$, the relative difference between the autocollimator's angle readings $\tilde{\alpha}$ and the tilt angle α is given by

$$\eta(c, D, f_0, p, p_0) = \frac{\tilde{\alpha} - \alpha}{\alpha} \approx c \cdot \left(\frac{D}{f_0} \right) \cdot (p - p_0) \,, \tag{5-1}$$

with the pressure sensitivity c

$$c(n_0, n_g, p_0) \approx \frac{n_0 - 1}{p_0 n_0} \left(\frac{n_g}{n_g - n_0} \right) \,. \tag{5-2}$$

The equations include the following parameters:

- D : Distance between the reflector and the autocollimator's objective.
- f_0 : Focal length of the autocollimator at the time of its assembly and adjustment by the manufacturer which has been stored in its electronics for calculating the measured angle. We

assume that the manufacturer carefully adjusts the imaging sensor to the focal plane of the objective under the environmental conditions at the time of assembly.

- p : Pressure during use of the autocollimator.
- p_0 : Pressure during the autocollimator's assembly and adjustment by the manufacturer.
- n_0 : Refractive index of the air during the autocollimator's assembly and adjustment.
- n_g : Refractive index of the bulk glass of the autocollimator's objective.

5.3 Pressure sensitivity of autocollimator measurements

In this section, we derive the pressure sensitivity c of the autocollimator's angle measurements theoretically and experimentally. From Equation (5-2), for the standard atmosphere at sea level, p_0 =1013.25 hPa, $(n_0 - 1) \approx 2.8 \cdot 10^{-4}$, and $n_g \approx 1.5$ for common optical glasses, we obtain $c \approx 0.83 \cdot 10^{-6}$ (arcsec/arcsec)/hPa, or 0.83 ppm/hPa (ppm: parts per million). Additionally, we performed ray trace modelling of the standard with Zemax, based on confidential design data kindly provided by the manufacturer, which result in $c \approx 0.82$ ppm/hPa.

To derive the pressure sensitivity c experimentally, we analysed PTB's extended set of monitoring calibrations of the standard. In Figure 5-1, for each calibration, the slope of a linear fit to the autocollimator' measuring deviations is plotted as a function of ambient air pressure. Horizontal bars characterise the standard deviations of the pressure changes during the acquisition of each calibration data set, vertical bars denote standard uncertainties of the slopes derived from the standard uncertainties of the respective deviations. A line fit (dashed, blue) results in $c \approx 1.28$ ppm/hPa. The distance of the reflector from the autocollimator was equal to its focal length, $D = f_0$ =300 mm. The pressure changes within each data set are quite substantial as each set consists of multiple repeat calibrations which require some time for their acquisition. They are performed in different relative orientations of the autocollimator with respect to the primary standard WMT 220 of PTB and in different directions of rotation (forward - backward). While it is possible to subdivide each calibration data set into its respective repeat calibrations, due to the absence of time stamps (we didn't consider pressure changes at that time), it is not feasible to assign pressure data to the repeats retroactively for achieving a better temporal resolution.

For a more precise experimental evaluation, the repeat calibrations needed to be performed more rapidly and correlated with pressure data logged concurrently. To this purpose, PTB's novel Spatial Angle Autocollimator Calibrator (SAAC) [5-4, 5-5] was used. To amplify the pressure influence, a reflector distance D =1700 mm was chosen, so that D / f_0 =5.67. From the data, $c \approx 0.95$ ppm/hPa can be derived. Three further data set, this time with $D = f_0$ =300 mm, demonstrate $c \approx 0.96$ ppm/hPa, 0.81 ppm/hPa, and 0.78 ppm/hPa, respectively. The investigation of several other autocollimators of the type used as the standard with the SAAC revealed consistent sensitivities. Because of the fast acquisition time (15 min) of each complete scan and the precise assignment of pressure data logged with high temporal resolution (5 min) to each scan, we deem these measurements and the resulting sensitivity much more reliable than the one derived from PTB's monitoring calibrations.

Further experimental data have been obtained with PTB's primary angle standard, the angle comparator WMT 220 [5-6 – 5-8]. Over a timespan of a week, the autocollimator was calibrated repeatedly, thus covering a pressure range of 15 hPa, which resulted in $c \approx 0.83$ ppm/hPa. In this case, in contrast to the monitoring calibrations mentioned above, the prompt assignment of pressure data

to each individual forward/backward measuring sequence was possible. The experimental results were corroborated by further investigations of the standard by Petr Kren, CMI, by use of their Interferometric Small Angle Generator (IGMU). He first pointed out, and experimentally investigated, the influence of air pressure on the autocollimator. Two data sets with $D = f_0$ =300 mm resulted in $c \approx$ 0.85 ppm/hPa and 0.77 ppm/hPa, respectively [5-9].

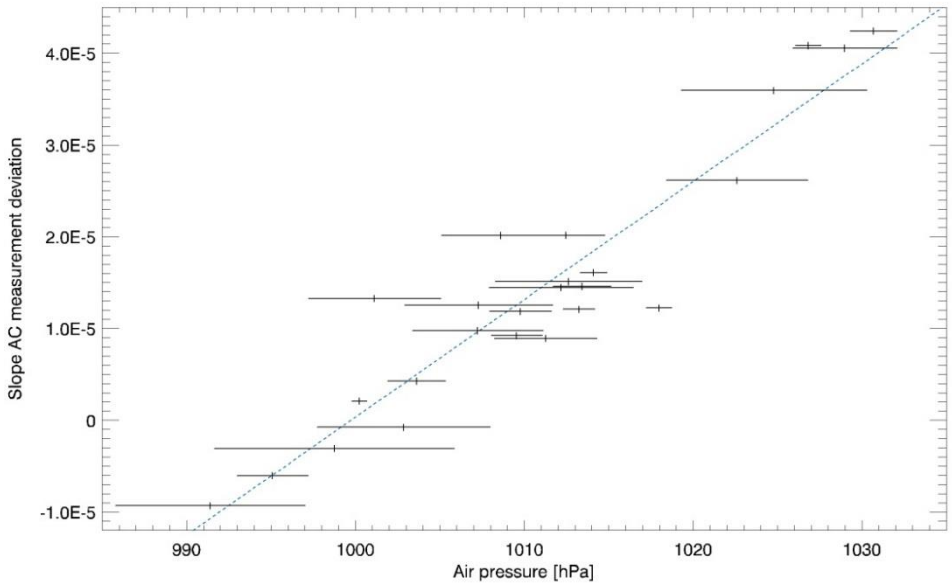

Figure 5-1. Pressure sensitivity of the standard's angle measuring deviations. For PTB's monitoring calibrations, the slope of a linear fit to each set of deviations is plotted as a function of air pressure. A line (dashed, blue) fitted to the data results in the sensitivity.

The values for the pressure sensitivity c of the standard obtained experimentally by use of PTB's SAAC, its WMT 220, and CMI's IGMU, the one derived by the analytical treatment, and the value obtained by ray trace modelling are quite consistent with each other. As noted, the value derived from PTB's set of monitoring calibrations is much less reliable due to the inability, at that time, to track rapid pressure changes and to correlate them with the standard's response at a high temporal resolution. For the analysis of the KC data, we use the weighted mean value derived from the SAAC data of c =0.91 ppm/hPa. We conservatively evaluate its associated standard uncertainty to be u_c =0.1 ppm/hPa.

5.4 Correcting pressure differences due to elevation

Air pressure decreases with increasing elevation above sea level. For deriving pressure as a function of the elevation H in the lower troposphere (H <11 km), we make use of the International Standard Atmosphere (ISA) [5-10]. For the correction of the influence of different elevations H on the autocollimator's angle measurements $\tilde{\alpha}$, we make use of Equation (5-1) and Equation (5-2):

$$\tilde{\alpha}(H_{ref}) = \tilde{\alpha}(H) - \eta(c, D, f_0, p(H), p(H_{ref})) \cdot \alpha \ . \qquad (5\text{-}3)$$

The correction achieves a referencing of the measurements obtained at an elevation H to a reference elevation H_{ref} and a reference pressure $p(H_{ref})$. A natural choice for H_{ref} is the elevation of the

manufacturer's lab where the autocollimator was assembled and adjusted. Table 5-1 presents the parameters for the correction as applied to the data of this comparison.

Table 5-1. Elevation correction of the participant's calibrations.

NMI	Country	Elevation H [m]	Pressure difference $p(H) - p(H_{ref})$ [hPa]	Reflector distance D [mm]	Elevation correction η [ppm] Eq. (5-3)	Type B uncertainty $\sqrt{\tilde{u}_\eta^2 + u_\eta^2}$ [ppm] Eq. (5-5)
A-Star	Singapore	49	-4.3	205	-2.7	9.9
BIM	Bulgaria	574	-65.5	300	-59.6	15.9
CEM	Spain	712	-81.1	300	-73.8	16.6
CMI-1	Czech Rep.	357	-40.6	200	-24.6	10.1
CMI-2	Czech Rep.	190	-21.1	300	-19.2	14.7
DMDM	Serbia	78	-7.8	160	-3.8	7.8
GUM	Poland	112	-11.8	300	-10.8	14.6
INM	Romania	87	-8.8	30	-0.8	1.5
INPL	Israel	784	-89.1	150	-40.6	8.5
INRIM	Italy	233	-26.1	300	-23.8	14.8
IPQ	Portugal	153	-16.7	350	-17.7	17.1
RCM-LIPI	Indonesia	65	-6.2	300	-5.7	14.6
LNE	France	62	-5.9	350	-6.2	17.0
METAS	Switzerland	546	-62.3	300	-56.7	15.8
MIKES	Finland	2	1.3	300	1.2	14.5
MKEH	Hungary	163	-17.9	300	-16.3	14.6
NIMA	Australia	2	1.3	300	1.2	14.5
NMI	China	49	-4.3	300	-3.9	14.5
NMIJ	Japan	26	-1.6	300	-1.4	14.5
NMIT	Thailand	3	1.2	300	1.1	14.5
NPL	United Kingdom	10	0.4	500	0.5	24.2
NPL	India	238	-26.7	300	-24.3	14.8
PTB	Germany	79	-7.9	300	-7.2	14.6
SMU-1	Slovak Rep.	218	-24.4	300	-22.2	14.7
SMU-2	Slovak Rep.	218	-24.4	500	-36.9	24.6
UME	Turkey	171	-18.8	300	-17.1	14.7
VNIIM	Russia	13	0.0	300	0.0	14.5
VSL	Netherlands	-2	1.8	300	1.6	14.5

5.5 Accounting for pressure variations due to weather

The influence of pressure differences due to the laboratories' different elevations can be corrected as described above. The substantial long- and short-term pressure variations due to weather changes need to be accounted for in a different way as the pressure was neither controlled nor recorded during the participants' calibrations. Pressure variations were not considered at the time when this KC was initiated and carried out; their significance became apparent only later. Their influence is evaluated, based on the analyses presented in the preceding sections, via a Type B uncertainty component [5-11] which was added to the uncertainty budgets provided by the participants.

From Equation (5-1), this Type B uncertainty component $\tilde{u}_\eta$ can be evaluated. By combining it with the standard uncertainty u_η due to the elevation correction of the autocollimator readings, see Equation (5-3), we obtain

$$\tilde{u}_\eta^2 + u_\eta^2 = \left(\frac{D}{f_0}\right)^2 \left\{ c^2\left(u_p^2 + u_{p_0}^2 + u_{p(H)}^2 + u_{p(H_{ref})}^2\right) + u_c^2 \left\{ (p-p_0)^2 + \left(p(H) - p(H_{ref})\right)^2 \right\} \right\}, \quad (5\text{-}4)$$

with the standard uncertainty u_c of the pressure sensitivity c, the standard uncertainty u_p of the air pressure $p(t)$ due to weather changes over time t, the standard uncertainty u_{p_0} of the air pressure p_0 during assembly and adjustment of the autocollimator by the manufacturer, the standard uncertainty $u_{p(H)}$ of the air pressure $p(H)$ due to the uncertainty u_H of the elevation H of the lab, and the standard uncertainty $u_{p(H_{ref})}$ of the air pressure $p(H_{ref})$ due to the uncertainty $u_{H_{ref}}$ of the reference elevation H_{ref}. Note that it is advisable to choose the elevation of the manufacturer's lab, where the autocollimator was assembled and adjusted, as the reference elevation H_{ref}.

We would like to note that the use of a common reference elevation H_{ref} and its associated reference pressure $p(H_{ref})$, as well as a common pressure p_0 during assembly and adjustment of the autocollimator, makes some comments on the derivations presented in the last two sections necessary. According to Equation (5-3), due to the use of a common $p(H_{ref})$, the corrections of the pressure differences due to different elevations of the participant's laboratories would have included a common component if – and only if – the same distance D between the reflector and the autocollimator would have been used by all participants. This common component would have re-appeared in the KCRV and would have cancelled out when evaluating the differences between the participant's results and the KCRV, as well as between each other (as is the case with the stable, intrinsic deviation of the standard). In case of our comparison, however, the participant's distances D did vary substantially between 30 mm and 500 mm. Nevertheless, the use of a common $p(H_{ref})$ effectively leads to a partial correlation between the elevation-corrections calculated for the participants and, therefore, between their elevation-corrected results. Similar considerations hold true when the influence of the varying ambient air pressure on the standard is evaluated which refers to a common pressure p_0 during assembly and adjustment of the autocollimator by the manufacturer.

The evaluation of the uncertainty components associated with the elevation correction and the influence of the unknown ambient air pressure according to Equation (5-4) neglects correlations. Effectively, Equation (5-4) *overestimates* the uncertainty components slightly and, therefore, provides a conservative *upper-limit* evaluation of them. When compared to an exhaustive evaluation, this results in slightly *smaller* E_N values, i.e., the degree of equivalence between each participant's result and the KCRV appears to be *better*. We decided to use this analytical expression of the uncertainty components nonetheless and to add them quadratically to the uncertainty budget provided by each participant. This procedure has the advantage of rendering the data analysis much more transparent and intelligible as it can follow the established rules for the evaluation of comparisons, including the use of intuitively understandable concepts, analytical expressions, and intermediate results. The alternative would have been a data evaluation based entirely on a front-to-end Monte Carlo approach. An evaluation of the procedure has demonstrated that it does not affect the conclusions of this Key Comparison. This has been achieved by using a *lower-limit* estimate of the uncertainty components according to Equation (5-4) by setting $u_{p(H_{ref})} = 0$ and $u_{p_0} = 0$ and by performing a complete re-analysis of the comparison. In other words, the use of both a lower-limit and upper-limit estimate of the uncertainty components results in outcomes of the comparison which are consistent with each other, with the exact solution being bounded by the two extrema.

Finally, we need to evaluate the input parameters to Equation (5-4) and derive its final expression.

u_p , u_{p_0} , and $\max|p-p_0|$: We analysed long-term (2006-2016) environmental data recorded at 5 min intervals at the clean room centre of PTB, where autocollimator calibrations are being performed. Over that decade, the values for the air pressure closely followed a normal distribution with a standard deviation of 9.2 hPa and a peak-to-valley range of 84 hPa. Please note that, due to the unstable weather conditions in northern Europe, these values are rather large. Geographical locations with more favourable, more stable environmental conditions may feature smaller values. Indeed, a few participants have provided such values. However, we decided to adopt this value as a conservative (i.e., upper limit) estimate and to apply it to the analyses of all participants' data sets uniformly (with the intent of avoiding to put the few participants which have provided pressure information at a disadvantage). From the available data, a standard uncertainty u_p =9.2 hPa can then be evaluated (with $p(t)$ obeying a normal distribution). As the air pressure during manufacturing and assembly of the autocollimator was not recorded either, $u_{p_0}=u_p$ follows. Here, p_0 is the air pressure during assembly and adjustment of the autocollimator by the manufacturer Möller-Wedel Optical, who is located near Hamburg, Germany, at an elevation H_{ref} of 13 m, while $p(t)$ is the air pressure due to weather changes over time t after its correction to the reference elevation H_{ref} . As the air pressures during assembly of the autocollimator and its use by the participants were not recorded, we need to provide a conservative estimate of $\max|p-p_0|$. We may assume that p_0 is located at the lower bound of the pressure range, while $p(t)$ covers pressure values up to the upper bound and vice versa. From the numbers cited above, we obtain $\max|p-p_0|$ =84 hPa.

$p(H)-p(H_{ref})$: The values of this parameter can be evaluated by use of the elevation data of the participants' laboratories and which are presented in Table 5-1, with $\max|p(H)-p(H_{ref})|$ =89 hPa for a reference elevation H_{ref} =13 m.

$u_{p(H)}$, $u_{p(H_{ref})}$: The standard uncertainties need to be evaluated from the uncertainties of the elevation data of the participant's laboratories and of the manufacturer and are estimated to be of the order of $u_H=u_{H_{ref}}$ =5 m at most. This results in $u_{p(H)}=u_{p(H_{ref})}$ =0.6 hPa.

u_c : With respect to the standard uncertainty u_c of the autocollimator's pressure sensitivity, we noted in Section 5.3 that we estimate it to be of the order of 0.1 ppm/hPa, with $c=0.91$ ppm/hPa.

By inserting the numbers provided above in Equation (5-4), we obtain the following numerical expression for the combined Type B uncertainty budget which will be added to the uncertainty budgets provided by the participants:

$$\sqrt{\tilde{u}_\eta^2+u_\eta^2}=10^{-6}\left(\frac{D}{f_0}\right)\left(211.3+0.01\cdot\left(\frac{p(H)-p(H_{ref})}{hPa}\right)^2\right)^{1/2} \qquad (5\text{-}5)$$

The numerical values are presented in Table 5-1. Please note that, according to Equation (5-1), this results in an uncertainty component $\sqrt{\tilde{u}_\eta^2+u_\eta^2}\cdot\alpha$ with respect to the standard's angle measuring deviations which increases linearly with the tilt angle α of the reflector and thus its angle readings.

5.6 References

[5-1] Geckeler RD, Kren P, Just A, Schumann M, and Krause M 2018 Influence of the air's refractive index on precision angle metrology with autocollimators *Meas. Sci. Technol.* submitted

[5-2] Edlén B The refractive index of air 1966 *Metrologia* **2** 71-80

[5-3] Birch KP and Downs MJ 1993 An updated Edlén equation for the refractive index of air' *Metrologia* **30** 155-162

[5-4] Geckeler RD, Kranz O, Just A, Krause M 2012 A novel approach for extending autocollimator calibration from plane to spatial angles *Advanced Optical Technologies* **1(6)** 427–39

[5-5] Kranz O, Geckeler RD, Just A, Krause M, and Osten W 2015 From plane to spatial angles: PTB's spatial angle autocollimator calibrator *Advanced Optical Technologies* **4(5-6)** 397-411

[5-6] Probst R, Wittekopf R, Krause M, Dangschat H and Ernst A 1998 The new PTB angle comparator *Meas. Sci. Technol.* **9** 1059-66

[5-7] Just A, Krause M, Probst R, Bosse H, Haunerdinger H, Spaeth C, Metz G and Israel W 2009 Comparison of angle standards with the aid of a high-resolution angle encoder *Precis. Eng.* **33(4)** 530-3

[5-8] Geckeler RD, Link A, Krause M, and Elster C 2014 Capabilities and limitations of the self-calibration of angle encoders *Meas. Sci. Technol.* **25** 055003 10pp

[5-9] Petr Kren 2015 (private communication, email from 13.11.2015)

[5-10] International Organization for Standardization: Standard Atmosphere (ISO 2533:1975)

[5-11] ISO/IEC Guide 98-3:2008 Guide to the Expression of Uncertainty in Measurement (ISO: 2008) (for the 1995 version with minor corrections, see JCGM 100:2008 http://www.bipm.org/en/publications/guides/gum.html)

6 Theory of data analysis

6.1 Measurement results

In general, the result of the calibration is the deviation δ of the angle α_{AC} measured by the standard, the autocollimator, from the angle α_{REF} provided by the reference system according to

$$\delta = \alpha_{\mathrm{AC}} - \alpha_{\mathrm{REF}} \,, \tag{6-1}$$

For the final calibration value δ, multiple repeat measurements may be obtained and processed, e.g., calibrations may be repeated in reverse directions to eliminate linear drifts. To eliminate arbitrary offsets between the participant's calibrations, from each set of deviations δ provided by the participants, its average was subtracted from all deviations comprising it.

6.2 Standard measurement uncertainty

The standard measurement uncertainty was evaluated according to the *Guide to the Expression of Uncertainty in Measurement* [6-1]. Alternatively, participants could choose to use the approach according to the *Supplement 1 to the GUM* [6-2] by propagating distributions (to obtain the Probability Density Function – PDF – of the output quantity from which an estimate of the output quantity itself, the standard uncertainty associated with it, and the coverage interval for a given coverage probability can be derived). In this section, the standard approach is outlined.

For each measured deviation δ, its associated standard uncertainty $u(\delta)$ was provided. For the derivation of the expanded uncertainty, the coverage factor k for a 95% coverage probability and, if appropriate, its effective degrees of freedom $\nu_{\mathrm{eff}}(\delta)$ were provided.

For deriving the uncertainty budget, the deviation $\delta = \alpha_{\mathrm{AC}} - \alpha_{\mathrm{REF}}$ of the autocollimator measurement from the measurement of the reference system, see Equation (6-1), needs to be expressed as a function of the N input quantities x_i, $i \in [1,...R]$, according to

$$\delta = f(x_1,...,x_i,...,x_R) \,. \tag{6-2}$$

Their uncertainty contributions $u_i(\delta)$ can be derived from the standard uncertainties $u(x_i)$ of the input quantities x_i as

$$u_i(\delta) = |c_i| \cdot u(x_i) \,, \tag{6-3}$$

with the sensitivity coefficients c_i according to

$$c_i = \frac{\partial \delta}{\partial x_i} \,. \tag{6-4}$$

The square of the combined standard uncertainty, $u^2(\delta)$, is derived from the quadratic sum of the uncertainty contributions, $u_i^2(\delta)$, according to

$$u^2(\delta) = \sum_{i=1}^{R} u_i^2(x_i) = \sum_{i=1}^{R} c_i{}^2 u^2(x_i) \ . \qquad (6\text{-}5)$$

In some cases, higher order terms have to be considered in Equation (6-5). If a correlation between the input quantities x_i is present, it also needs to be considered:

$$u^2(\delta) = \sum_{i=1}^{R}\sum_{l=1}^{R} c_i c_l \cdot u(x_i, x_l) = \sum_{i=1}^{R} c_i{}^2 u^2(x_i) + 2\sum_{i=1}^{R-1}\sum_{l=i+1}^{R} c_i c_l \cdot u(x_i, x_l) \ , \qquad (6\text{-}6)$$

with the covariances $u(x_i, x_l)$ associated with the input quantities x_i and x_l, $i,l \in [1,...R]$.

For the uncertainty estimation, the participants were encouraged to use all known and significant influencing parameters associated with their method of calibration. For documentation, the participants were required to report their measurement uncertainty budget in tabular format.

6.3 Comparison / analysis of results

According to the MRA, the main objective of a comparison is to provide reliable information on the degree of equivalence of the different angle realizations between the participating laboratories. To accomplish this, the calibration results of the participants, which are given as deviations δ of the angles measured by the standard from the angles provided by the reference system, have to be analysed further. The following procedure for analysing the comparison results was implemented, closely following the recommendations outlined in [6-3].

6.3.1 Input data

Input data are the calibration values delivered by the participants, specifically:

- The deviations $\delta_{jp} = \alpha_{\mathrm{AC},jp} - \alpha_{\mathrm{REF},jp}$ of the angles $\alpha_{\mathrm{AC},jp}$ measured by the standard from the angles $\alpha_{\mathrm{REF},jp}$ provided by the reference systems, with the index $j \in [1,...,N]$ of the angle position and the participant's index $p \in [1,...,M]$.
- The combined standard uncertainties $u(\delta_{jp})$ associated with the deviations δ_{jp}.

6.3.2 Key Comparison Reference Values (KCRV)

The Key Comparison Reference Values (KCRV) were generated from the participants' results. It is assumed that each participant's measurement of the standard is realized independently of the other participants' measurements, and that a Gaussian distribution (with a mean equal to the participant's measurement and a standard deviation equal to the associated standard uncertainty) can be assigned to the measurand of which the participant's measurement is an estimate. The later will also be checked, see Section 6.3.3.

As noted in Section 5, the standard (i.e., the autocollimator) proved to be influenced by environmental factors which were - due to our lack of knowledge on this influence at that time - neither controlled

nor recorded during the comparison. An elaborate analysis of these influences was provided in the section and it was accounted for by adding appropriate Type B uncertainty components to the uncertainties provided by each participant.

Each reference angle deviation $\tilde{\delta}_j$, the KCRV, is given by the weighted mean of the participants' results, with the weights defined by the inverse squares of the standard uncertainties, $u^{-2}(\delta_{jp})$, according to

$$\tilde{\delta}_j = \frac{\sum_{p=1}^{M} u^{-2}(\delta_{jp}) \cdot \delta_{jp}}{\sum_{p=1}^{M} u^{-2}(\delta_{jp})} \quad . \tag{6-7}$$

Along the lines of Equations (6-3) – (6-7), we can derive the sensitivity coefficients

$$c_{jp} = \frac{\partial \tilde{\delta}_j}{\partial \delta_{jp}} = \frac{u^{-2}(\delta_{jp})}{\sum_{p=1}^{M} u^{-2}(\delta_{jp})} \tag{6-8}$$

and the standard uncertainty (assuming uncorrelated measurements)

$$u(\tilde{\delta}_j) = \left(\sum_{p=1}^{M} c_{jp}^2 \cdot u^2(\delta_{jp}) \right)^{1/2} = \left(\sum_{p=1}^{M} u^{-2}(\delta_{jp}) \right)^{-1/2} . \tag{6-9}$$

Note that there is a small subset of participants which were not able to perform the calibrations according to the recommendations on the measurement ranges and steps given in Section 4. In these cases, the participant's data sets were interpolated appropriately to conform to the specified sampling.

6.3.3 Birge ratio

The Birge ratio is a parameter linked to the χ^2 test and it allows estimating whether the results of a comparison are consistent [6-4 – 6-6]. With the external and internal uncertainties of the weighted mean, u_{ext} and u_{int}, respectively, defined as

$$u_{\text{ext},j} = \left(\frac{1}{M-1} \frac{\sum_{p=1}^{M} u^{-2}(\delta_{jp}) \cdot \left(\delta_{jp} - \tilde{\delta}_j\right)^2}{\sum_{p=1}^{M} u^{-2}(\delta_{jp})} \right)^{1/2} \quad \text{and} \tag{6-10}$$

$$u_{\text{int},j} = u(\tilde{\delta}_j) \ , \tag{6-11}$$

the Birge ratio $R_{\mathrm{B},\,j}$ is given as

$$R_{\mathrm{B},\,j} = \frac{u_{\mathrm{ext},\,j}}{u_{\mathrm{int},j}} = \left(\frac{1}{M-1} \sum_{p=1}^{M} u^{-2}(\delta_{jp}) \cdot \left(\delta_{jp} - \tilde{\delta}_j\right)^2 \right)^{1/2} . \qquad (6\text{-}12)$$

Under the assumptions cited in Section 6.3.2, the values $(M-1)R_{\mathrm{B},\,j}^2$ follow a χ_{M-1}^2 distribution with the degree of freedom $\nu = M-1$. The expectation value of $R_{\mathrm{B},\,j}$ is then 1. A Birge ratio $R_{\mathrm{B},\,j}$ significantly larger than one is indicating an underestimation of the measurement uncertainty by at least one participant. Following [6-3], we regard this consistency check as having failed if $(M-1)\cdot R_{\mathrm{B},\,j}^2 > \chi_{M-1}^2(0.95)$.

6.3.4 Differences from reference values

From the participants' measurements, differences $\Delta\delta_{jp}$ from the KCRV are calculated according to

$$\Delta\delta_{jp} = \delta_{jp} - \tilde{\delta}_j \qquad (6\text{-}13)$$

and their associated uncertainties $u(\Delta\delta_{jp})$ are evaluated according to

$$u(\Delta\delta_{jp}) = \left(u^2(\delta_{jp}) + u^2(\tilde{\delta}_j) - 2u(\delta_{jp}, \tilde{\delta}_j)\right)^{1/2} , \qquad (6\text{-}14)$$

with the covariance or mutual uncertainty $u(\delta_{jp}, \tilde{\delta}_j)$ [6-1] which accounts for the correlation between the participants' measurements δ_{jp} and the reference values $\tilde{\delta}_j$ which have been derived from them. Most participants provided measurements which were used for deriving the reference values. In those cases, $u(\delta_{jp}, \tilde{\delta}_j) = u^2(\tilde{\delta}_j)$. For measurements which were not included, $u(\delta_{jp}, \tilde{\delta}_j) \equiv 0$ is valid, based on their full independence from the reference values. Using Equation (6-7), Equation (6-14) can then be expressed as

$$u(\Delta\delta_{jp}) = \begin{cases} \left(u^2(\delta_{jp}) - u^2(\tilde{\delta}_j)\right)^{1/2} & \text{participant did contribute to KCRV} \\ \left(u^2(\delta_{jp}) + u^2(\tilde{\delta}_j)\right)^{1/2} & \text{participant did not contribute to KCRV} \end{cases} . \qquad (6\text{-}15)$$

6.3.5 Degree of equivalence (DoE)

The E_{N} criterion is proposed to give information on the degree of equivalence of the different angle realizations of the participants, e.g. [6-7, 6-8]. With respect to the differences $\Delta\delta_{jp}$ from the KCRV according to Equation (6-13), the definition of the $E_{\mathrm{N},\,jp}$ is

$$E_{\mathrm{N},\,jp} = \frac{1}{k}\frac{\Delta\delta_{jp}}{u(\Delta\delta_{jp})}\ , \tag{6-16}$$

with the coverage factor k according to [6-1] and the standard uncertainty $u(\Delta\delta_{jp})$ according to Equation (6-15). Usually, the compatibility criterion $|E_{\mathrm{N}}| \le 1$ is proposed to indicate that the measurement of a participant is in satisfactory agreement, at 95% coverage probability, with the KCRV.

6.3.6 Supplemental Monte Carlo approach

For a refined analysis, we utilised a Monte Carlo (MC) approach to simulate the deviations δ_{jp} of the standard, as realised by the participants' measurements, which are expected when all available prior knowledge is used. This includes the standard uncertainties $u(\delta_{jp})$ associated with the δ_{jp}, which were provided by the participants. Additionally, the pressure influence was modelled as realistically as possible by use of the functionalities as well as the parameter ranges and distributions provided in Section 5. The simulated deviations δ_{jp} were then fed through the same data analysis algorithms which were used to analyse the experimental data sets.

The advantage of this MC approach is that it provides not only expectation values for the various analysis results and measures, but also their probability density functions (all within the limits of the available prior knowledge). These allow us to compare the experimental results to the simulated MC-based results in detail and to evaluate the significance of deviations between the two more accurately.

From the measurements of the standard provided by each participant $p \in [1,\ldots,M]$ at multiple sampling points $j \in [1,\ldots,N]$, the $E_{\mathrm{N},\,jp}$ values are derived according to Equation (6-16). As noted, the MC approach described above allows us to evaluate the measured values, $E_{\mathrm{N},\,jp}$, in the light of the distributions which result from the simulated values, $E^{\mathrm{MC}}_{\mathrm{N},\,jps}$, where $s \in [1,\ldots,S]$ is the index of the MC realisation. We consider the set of measurements provided by a participant p at the sampling points j as the basis for a multiple testing of the null hypotheses that the measured $E_{\mathrm{N},\,jp}$ are derived from the MC-based distributions of the $E^{\mathrm{MC}}_{\mathrm{N},\,jps}$. To this purpose, we apply the Bonferroni correction to this multiple hypothesis testing [6-9, 6-10]. It has the advantage that it does not require any assumptions on how many null hypotheses are true or whether any dependence between them exists.

For each participant p, we derive the probabilities q_{jp} for $\left|E^{\mathrm{MC}}_{\mathrm{N},\,jps}\right| > \left|E_{\mathrm{N},\,jp}\right|$ at the sampling points j. We require that the probability of falsely rejecting at least one true null hypothesis, i.e., of making an (Type I) error in judgment when testing, is not larger than 5% (i.e., we require that the familywise error rate – FWER – is smaller than 5%). By following the Bonferroni correction, we reject the null hypothesis associated with each sampling point j if

$$q_{jp} \le \frac{0.05}{N}\ , \tag{6-17}$$

where N is the number of sampling points measured by the participant. For each participant p, we require that not a single null hypothesis associated with the sampling points $j \in [1,\ldots,N]$ is rejected according to the criterion presented in Equation (6-17).

We would like to note that this criterion is only one of multiple measures which are used judiciously to evaluate the consistency of the participants' measurements of the standard and their degree of equivalence to the KCRV. If significant deviations were detected, the participants were informed and the recommendations of the *Guidelines for CIPM Key Comparisons* [6-11] were followed.

6.4 References

[6-1] ISO/IEC Guide 98-3:2008 Guide to the Expression of Uncertainty in Measurement (ISO: 2008) (for the 1995 version with minor corrections, see JCGM 100:2008 http://www.bipm.org/en/publications/guides/gum.html)

[6-2] JCGM 101:2008 "Evaluation of measurement data - Supplement 1 to the 'Guide to the expression of uncertainty in measurement' - Propagation of distributions using a Monte Carlo method" Joint Committee for Guides in Metrology (JCGM: 2008) http://www.bipm.org/en/publications/guides/gum.html

[6-3] Cox MG 2002 The evaluation of key comparison data *Metrologia* **39** 589-595

[6-4] Birge RT 1932 The calculation of errors by the method of least squares *Phys. Rev.* **40** 207-227

[6-5] Kacker R, Datla R, and Parr A 2002 Combined result and associated uncertainty from interlaboratory evaluations based on the ISO Guide *Metrologia* **39** 279-293

[6-6] Bodnar O and Elster C 2014 On the adjustment of inconsistent data using the Birge ratio *Metrologia* **51** 516-521

[6-7] Wöger W 1999 Remarks on the En-criterion used in measurement comparisons *PTB-Mitteilungen* **109(1)** 24-27

[6-8] Beissner K 2002 On a measure of consistency in comparison measurements *Metrologia* **39** 59-63

[6-9] Bonferroni CE 1935 Il calcolo delle assicurazioni su gruppi di teste *Studi in Onore del Professore Salvatore Ortu Carboni* 13-60

[6-10] Bonferroni CE 1936 Teoria statistica delle classi e calcolo delle probabilità *Pubblicazioni del R Istituto Superiore di Scienze Economiche e Commerciali di Firenze* **8** 3-62

[6-11] Guidelines for CIPM key comparisons (CIPM: 1999), http://www.bipm.org/en/cipm-mra/guidelines_kcs/

7 Experimental results and analysis

7.1 Participant's measuring conditions

Due to the large number of participants involved in this KC, we provide an overview of the participants' measuring conditions in Table 7-1.

Table 7-1. Measuring conditions. The abbreviations SR and LR denote the small measuring range (± 10 arcsec) and the large measuring range (± 1000 arcsec), respectively.

NMI	Measuring conditions					Meas. mode	Measurement procedure				
	Orient. AC x-axis	Added optics	Plane mirror	Dist.	Temp.	Manual Text / Compatible mode of RS 232 interface	Static or dyn. meas.	n_i	Rel. ori.	n_{AC}	n_{REF}
	Horiz. Vertical	Yes No	By PTB / NMI	[mm]	[°C]		Static Dyn.		Yes No		
INM	LR: H SR: V	N	PTB	30	20.5	M 0.001 arcsec		12	N	1	1
INRIM	V	N	PTB	300	20.0±0.5	T	S	17	Y	10	1
LNE	H	N	PTB	350	n.a.	T	S	10	N	50	1
METAS	H		PTB	300	19.8±0.2	T	S	5	N	100	1
MIKES	H	N	NMI	300	19.97±0.05	T	S	LR: 12 SR: 8	N	100	50
NPL	H	N	PTB & NMI	300	20.0	C	S	30	N	80	8000
UME	H	N	PTB & NMI		20.0±0.2	T	S	LR: 12 SR: 30	Y	50	50
VSL	V	N	PTB	300	20.0±0.5	M 0.01 arcsec	S	3	N	1	1
CEM	H	N	PTB	300	20.0±0.5	n.a.	S	2	Y	5	5
CMI-1	H	N	PTB	200	20.0±0.5	T	S	9	Y	40	40
CMI-2	H	N	NMI	300	20.0	T	S	10	N	60	60
GUM	H	N	PTB & NMI	300	20.0±0.5	T	S	9	Y	LR: 60 SR: 50	1
INPL	H	N	PTB	150	20.0±0.5	M 0.02 arcsec	S	20	Y	n.a.	n.a.
IPQ	H	N	PTB	350	20.3±0.5	T	S	8	Y	10	10
MKEH	V	N	NMI	300	20.03	T	S	6	N	1	1
SMU-1	H	Y Penta prism	NMI	300	21.5	T	S	SR: 15 LR: 30	N	300	300
SMU-2	V	N	NMI	500	24.0	T	S	12	Y	100	100
NMI (China)	H	N	PTB	300	20.0±0.2	T	S	20	N	50	50
NIMA	V	N	PTB	300	20.2±0.2	M 0.01 arcsec	S	6	Y	1	1
NMIJ	H	N	PTB	300	20.0±0.1	T	S	20	Y	200	225000
NPL (India)	H	N	PTB	500	20.0±0.5	M 0.01 arcsec	S	3	N	10	10
A-Star	V	N	NMI	205	19.8	T	S	LR: 5 SR: 3	N	200	200
BIM	V	N	PTB	300	20.0±0.5	M 0.001 arcsec	S	4	Y	25	25
DMDM	H	N	PTB	160	20.0±0.5	T	S	2	N	100	19
RCM-LIPI	H	N	PTB	300	20.0±0.3	T	S	3	Y	100	10
NIMT	H	N	PTB	300	20.0±1	T	D	20	Y	100	10
VNIIM	H	N	PTB	300	20.0±0.3	T	S	LR: 6 SR: 1	N	50	LR: 10 SR: 40
PTB	H	N	PTB	300	20.0±0.05	T	S	10	Y	100	25

From left to right, the columns present information on:

- the acronym of the NMI,
- the orientation of the autocollimator axis to be calibrated (the x axis),
- whether additional optics for beam deflection were used in the calibration set-up,
- which plane mirror was used, the one owned by the NMI or the one supplied by PTB,
- the distance between the reflecting mirror and the front of the autocollimator's objective,
- the temperature during calibration,
- the autocollimator measuring mode: manual measurements or automated measurements by use of the autocollimator's RS 232 interface and the two available data transfer protocols, text and compatible,
- whether static (stop-and-go) or dynamic measurements were performed,
- the number of repeat calibrations n_i which were averaged,
- whether different relative angular orientations between the autocollimator and the calibration set-up were used,
- the number of autocollimator readings n_{AC} which were averaged at each sampling point,
- the number of readings of the reference system n_{REF} which were averaged at each sampling point.

A few participants used their own plane mirrors for their calibrations on which they provided the following specifications:

- A-Star: Reflectivity 96%; diameter 45 mm; flatness deviation 60 nm pv
- CMI-2: Reflectivity 95%; diameter 50 mm; flatness deviation 5 nm pv over d=30 mm
- NPL: Reflectivity n.a.; diameter n.a; flatness deviation 22 nm ± 20 nm
- MIKES: Reflectivity 95%; diameter 50 mm; flatness deviation 30 nm pv
- MKEH: Reflectivity 99%; diameter 48 mm; flatness deviation <200 nm pv
- SMU: Reflectivity 95%; diameter 50 mm; flatness deviation n.a.
- UME (LR): Reflectivity 96%; size 45 mm x 70 mm; flatness deviation 8 nm rms, 40 nm pv
- UME (SR): Reflectivity 99%; diameter 50 mm; flatness deviation 3 nm rms, 25 nm pv

7.2 Damage and repair of the standard

The standard suffered transport damage early in the KC during its distributions in Loop 1. By comparing the extended monitoring calibrations performed at the pilot lab PTB and the calibrations of the different participants, the damage could be located in time.

The monitoring calibrations performed in December 2009 and May 2010 were consistent with each other. In contrast, the next monitoring calibration performed in November 2010 showed an inconsistency of approx. 0.047 arcsec pv (peak-to-valley) and 0.011 arcsec rms (root-mean-squared) over the entire measuring range of ±1000 arcsec. Note that it fits well within the specifications for the device stated by the manufacturer (±0.25 arcsec over the entire measuring range) and would have been, due to the participants' uncertainties, not detectable by many of the participants.

Between May and November 2010, four participants performed calibrations of the standard (INRiM, UME, INM, and LNE), see Table 3-2, Section 3.3. The participants were informed of the damage and, after the repair of the standard, were offered the option to repeat their calibrations. Only INRiM

performed a re-calibration. PTB intensified its extensive monitoring calibrations during the entire comparison to detect further damage.

The standard was sent to its manufacturer, Möller-Wedel Optical, and refurbished in February 2011. It was determined that there was a loosening of the autocollimator's objective (which had never been observed before) due to the exceptional mechanical stresses during transportation.

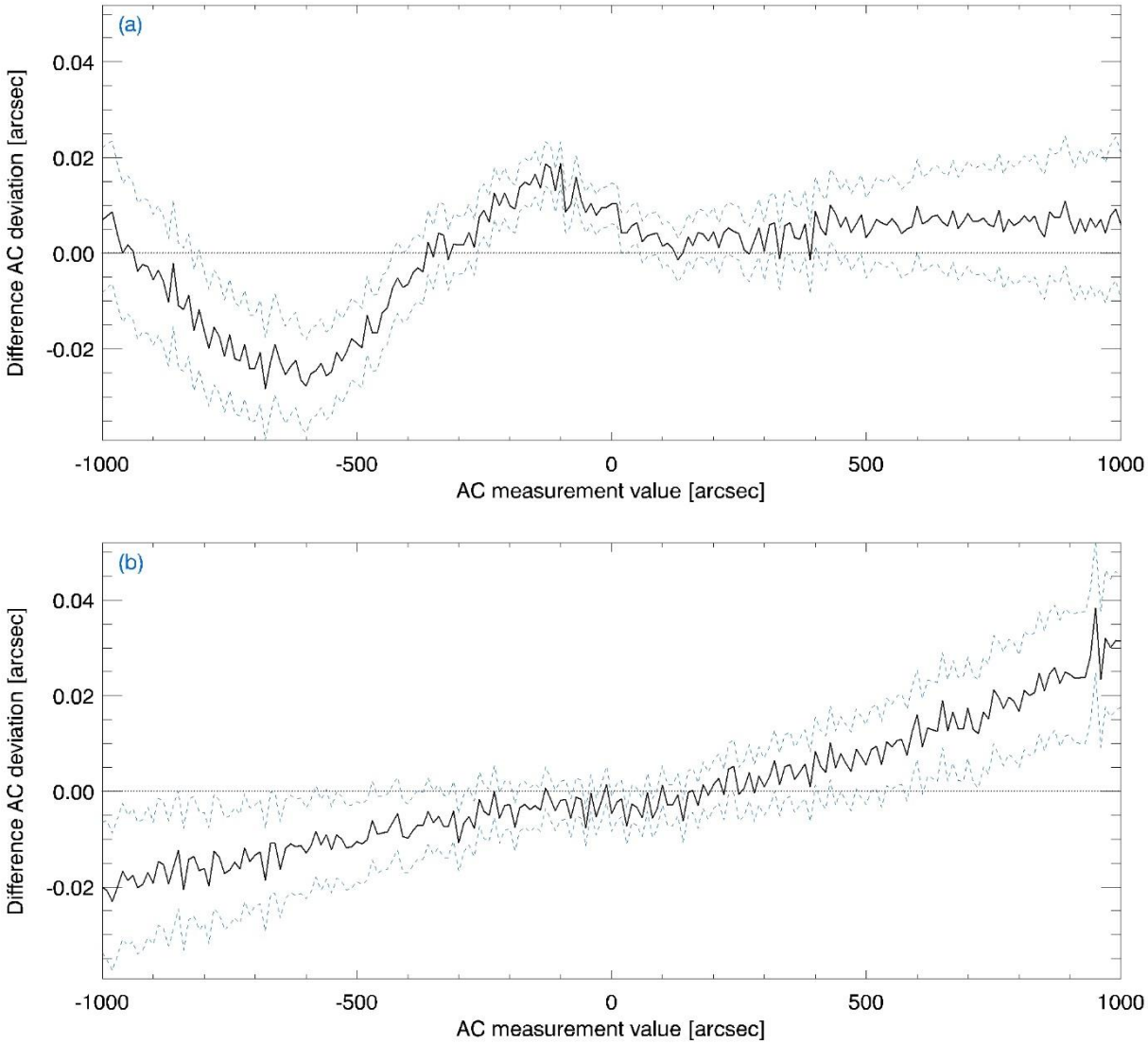

Figure 7-1. (a) Difference between the standard's measuring deviations before and after the transport damage. (b) Difference between the standard's measuring deviations before transport damage and after its repair. Additional lines (dashed, blue) mark the ranges given by the associated standard uncertainties which include the influence of the air pressure.

Figure 7-1(a) demonstrates the impact of the transport damage on the standard. It presents the difference between the standard's measuring deviations before and after the occurrence of the damage as derived from PTB's monitoring calibrations (solid, black line). The graph includes additional lines (dashed, blue) which mark the range given by the associated standard uncertainties for the difference values which include a component due to the unknown air pressure.

Figure 7-1(b) demonstrates the impact of the repair of the standard by the manufacturer. It presents the difference between the standard's measuring deviations before the occurrence of the transport damage and after its repair as derived from the two sets of KCRV values for the full measuring range (solid, black line). Again, additional lines (dashed, blue) mark the range given by the associated standard uncertainties for the values with the range derived from the associated standard uncertainties of the two data sets. The repair eliminated the higher-order measuring deviations while introducing a linear component, most probably caused by minor differences in the adjustment of the distance of the autocollimator's objective to the CCD detector.

We would like to stress again that both the impact of the transport damage and of the repair on the standard's measuring deviations

(1) are barely detectable at the level of the extended measurement uncertainty (95% coverage probability), if the component due to the unknown air pressure is included properly,

(2) fit within the specifications for the device stated by the manufacturer, and

(3) are below the significance threshold of detectability for most the participants.

Due to the occurrence of the transport damage to the autocollimator and its subsequent repair by the manufacturer, we treated the autocollimator before and after the repair as independent standards. Therefore, we split the participants' data sets accordingly into two groups and analysed them separately. These groups of data sets are referred to as

- S1 (standard before repair) and
- S2 (standard after repair).

Additionally, we split the data sets per the two measuring ranges into

- SR (small measuring range, ± 10 arcsec) and
- LR (large measuring range, ± 1000 arcsec).

PTB has analysed its extended set of monitoring measurements of the standard which were performed above and apart of the measurements listed in Table 3-2, Section 3.3. We have verified that the monitoring measurements within each subset S1 & S2 are consistent with each other if the uncertainty component due to the influence of the unknown air pressure is accounted for as described in Section 5.

7.3 Inclusion criteria for KCRV

Concerning the calibrations obtained by the participants with the standard S1 (before repair), due to the damage of the standard during Loop 1, the calibrations which were included in the KCRV had to be chosen with care. Only those calibrations were included in the KCVR which were measured at dates between the two monitoring measurements of PTB which showed no indication of the transport damage. This selection criterion was applied to make sure that the participants' calibrations were obtained before the damage. Note that this criterion implies that some calibrations had to be excluded from the KCRV which were not conspicuous with respect to their E_{N} values. In the case that participants provided calibrations by use of their own mirror and the one supplied by PTB, only the former was included in the KCRV. The reason behind this selection is to validate the set-up at the NMI commonly used for autocollimator calibration and to avoid over-representation of the NMI in the KCRV.

In case of the data set S1-LR (standard S1 before repair; large measuring range of ±1000 arcsec in steps of 10 arcsec), the following participants have been excluded from the KCRV: NPL (data set obtained with PTB mirror), LNE, INM, and UME. In case of the data set S1-SR (standard S1 before repair; small

measuring range of ±10 arcsec in steps of 0.1 arcsec) the following participants have been excluded: NPL (data set obtained with PTB mirror), INM, and UME.

Concerning the data set obtained with the standard S2 (after repair), a first analysis was performed which included all participants. KCVR values, E_N values, and Birge ratios were calculated. Based on the E_n values, an iterative standard approach was carried out with respect to those participants for which these values were conspicuous. The participant with the largest number of values $|E_N| > 1$ was excluded from the KCVR calculation and the KCVR, E_N, and Birge ratios values were then re-calculated. The process was repeated until a consistent selection of data sets for the KCVR was achieved. For details on the E_N values which guided our selection, see Section 7.4.

In case of the data set S2-LR (standard S2 after repair; large measuring range of ±1000 arcsec in steps of 10 arcsec), the following participants have been excluded from the KCRV: GUM, RCM-LIPI, MKEH, CMI (data set CMI-2 only). The latter data set (CMI-2) was excluded not due to conspicuous E_N values, but because it resulted from an adjunct comparison with a novel calibration set-up at CMI. It was not part of the original KC, in contrast to the data set CMI-1. In case of the data set S2-SR (standard S2 after repair; small measuring range of ±10 arcsec in steps of 0.1 arcsec) the following participants have been excluded: VNIIM and CMI (data set CMI-2 again).

In the case that values (measurement values, uncertainties, etc.) were revised by participants, the latest versions of the values were used for this analysis. See also the comments of participants provided in Section 8. To provide uniform data sets for the analysis, each participant's set of autocollimator deviations was handled in the following way: From all autocollimator deviations belonging to the set, the average value (calculated from the deviations) was subtracted. This ensures that no systematic offsets between the data sets are present.

As the pilot laboratory, PTB performed many monitoring calibrations of the autocollimator during this KC. They provided valuable information on the long-term stability of the autocollimator and were included in the data analysis and the final report on the comparison presented here. To avoid a selection of PTB's reference calibrations from this large database based on questionable criteria which might bias our results, we chose the following procedure: For each loop, PTB's reference calibration was identified with the calibration which was performed immediately before sending the autocollimator out of PTB, i.e., the calibration performed immediately before the start of each loop.

7.4 Results

7.4.1 Results for standard S1 – small measuring range SR

Figure 7-2 presents the data relevant to the KCRV. Data are presented for measurements performed by use of the standard S1 (before repair) over the small measuring range (SR) of ± 10 arcsec (data set S1-SR).

Figure 7-2(a) presents the KCRV values (solid, black line). The graph includes additional lines (dashed, blue) which mark the range given by the associated standard uncertainties for the KCVR values which are also presented separately in Figure 7-2(b). The dips in the standard uncertainties are because, depending on the coverage of the sampling points by the participants, different numbers of data points were available for each KCRV value. These numbers are shown in Figure 7-2(c).

Figure 7-3 presents data characterising the deviations of the participants' calibrations from the KCRV. Due to the large number of participants involved in this KC, we opted for a compact visualisation of the results. Additionally, individual graphs for each participant are provided in Figure 7-4. Note also that we characterise the deviations by use of the E_N values solely. Due to the substantial spread of the calibration uncertainties stated by the large number of participants, it is not useful to refer to the absolute deviations.

Figure 7-3(a) presents a review of the deviations of the participants' calibrations from the KCRV, characterised by E_N values, as a compact box plot. Each rectangular box visualises the average E_N (bar at the centre of the box) and the range given by one standard deviation of the E_N values (upper margin of the box: average plus one standard deviation; lower margin: average minus one standard deviation), while the remaining bars denote the full range of the E_N by marking the minimal and maximal values. The values $E_N = \pm 1$ (dashed, blue lines) are highlighted.

Figure 7-3(b) presents the standard deviations of the E_N values which were used for the box plot (solid, black line). Additionally, the limits for the standard deviations are shown (dashed, blue line) which were derived by use of the Monte Carlo approach outlined in detail in Section 6.3.6. The line marks the upper limit below which 95% of the simulated values for the standard deviations of the E_N are located. In case that a participant's value violates this limit (i.e., that the value exceeds the limit), it is marked by an asterisk. Please note the prevalence of standard deviations of the E_N values which are substantially smaller than 0.5. This is caused by the fact that the uncertainty component due to the influence of the unknown air pressure during calibration needed to be estimated conservatively by evaluating the maximal pressure changes prevalent across the geographical locations of the participants' laboratories. As noted in Section 5, some labs are located at places which may feature more stable pressures which vary within smaller ranges.

Figure 7-3(c) presents the fraction of values for which $|E_N| > 1$ (solid, black line). Additionally, the limits for the fractions are shown (dashed, blue line) which were derived by use of the MC approach. Again, the line marks the upper limit below which 95% of the simulated values are located; violations of the limit are marked by an asterisk.

Table 7-2 presents the data visualised in Figure 7-3 in tabular form. Additionally, in its third column, it presents the initial standard measurement uncertainty supplied by each participant at the margin of the angular measuring range (i.e., α = 10 arcsec in case of the small range and α = 1000 arcsec in case

of the large range). In the fourth column, the corrected uncertainty is presented after accounting for the uncertainty components associated with the elevation correction and the influence of the unknown ambient air pressure, see Section 5.5, Equation (5-5). Note that a substantial difference between both uncertainties is only discernible in case of a large measuring range and, due to the combination of the uncertainty components by quadratic addition, a low initial uncertainty.

We would like to stress that the multiple measures presented in the graphs need to be used judiciously to evaluate the consistency of the participants' measurements of the standard and their degree of equivalence to the KCRV. For some participants, multiple measures indicate significant mismatches between the deviations from the KCRV and the stated uncertainties which need explanation and warrant further investigation. This is the case for UME (see also the detailed comments in Section 8).

Please note that the measurements of the standard provided by NPL were obtained by use of the 'Compatible' mode of the autocollimator's RS 232 interface. This was the case for all measurements which NPL contributed to the S1-SR and the S1-LR data sets. PTB noticed that there is a problem with this mode when compared to the 'Text' mode (which was used by all other participants which made use of an automated autocollimator readout). The measurements provided by the interface in the 'Compatible' mode are affected by an asymmetrical rounding error: positive angle readings are shifted by 0.005 arcsec, while negative angle readings are shifted by the same amount, but in the opposite direction. This leads to a total systematic shift between positive and negative angle readings of 0.01 arcsec. To our knowledge, this is the first time that this effect has been observed with this type of autocollimator and it may be specific to the software version used with this individual autocollimator. Therefore, prior to the data analysis, PTB had to correct this systematic error in NPL's measurements of the standard.

Table 7-2. Deviations of the participants' calibrations from the KCRV for data set S1-SR.

NMI	Country	Initial std. unc. α = 10″ [arcsec]	Corrected std. unc. α = 10″ [arcsec]	Std. dev. E_N	Range E_N [min., max.]	Fraction [%] $\lvert E_N \rvert > 1$
INM	Romania	0.050	0.050	0.13	[-0.23, 0.42]	0.0
MIKES	Finland	0.009	0.010	0.16	[-0.36, 0.30]	0.0
PTB	Germany	0.003	0.003	0.35	[-0.86, 1.07]	0.5
NPL-1[a]	United Kingdom	0.005	0.005	0.37	[-1.12, 0.89]	1.0
NPL-2[a]	United Kingdom	0.004	0.004	0.38	[-0.81, 0.86]	0.0
UME	Turkey	0.005	0.005	0.92	[-1.64, 1.79]	38.8

a: Calibrations were obtained by use of different mirrors.

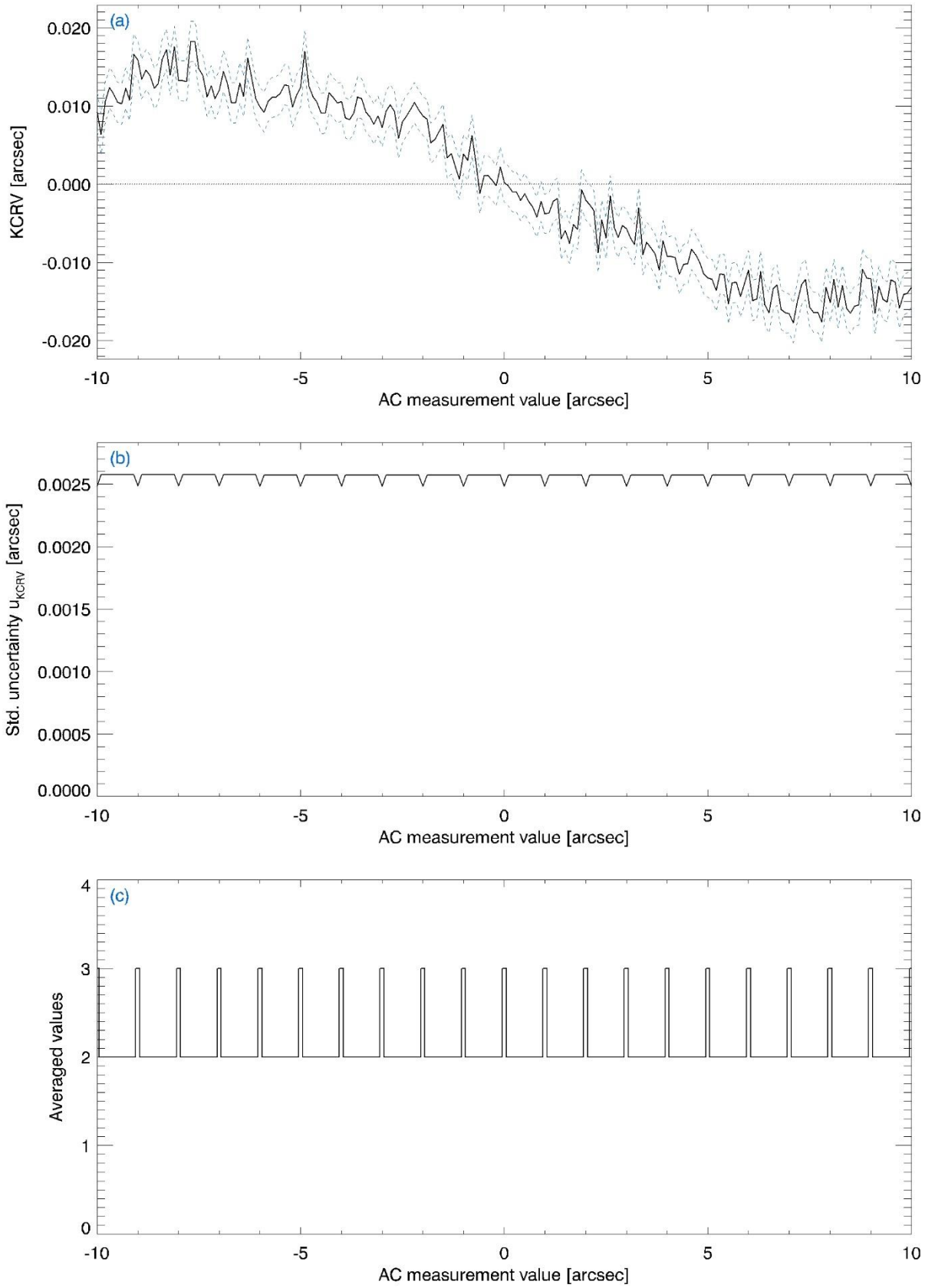

Figure 7-2. Data set S1-SR: (a) KCRV values (solid, black line) and the range (dashed, blue lines) given by the associated standard uncertainties. (b) Standard uncertainties of the KCRV values. (c) Number of participants included in KCRV values (due to the differing sampling of the participants).

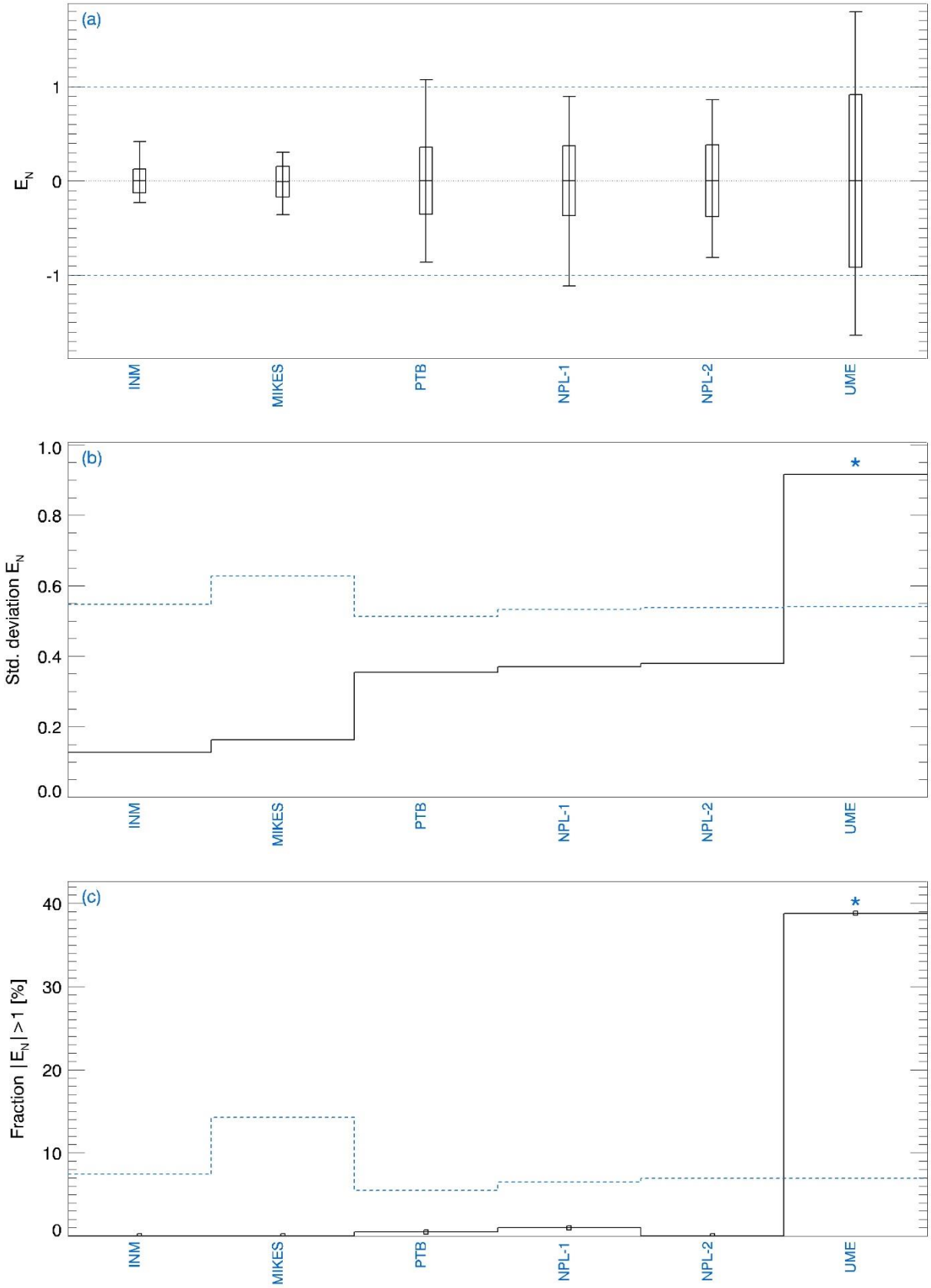

Figure 7-3. Data set S1-SR: Deviations of the participants' calibrations from the KCRV. (a) Box plots of the E_N values, see text for details. (b) Standard deviations of the E_N values (solid, black line) and MC-based upper limits associated with a 95% coverage probability (dashed, blue line). (c) Fraction of values $|E_N| > 1$ (solid, black line) and 95% upper limits (dashed, blue line).

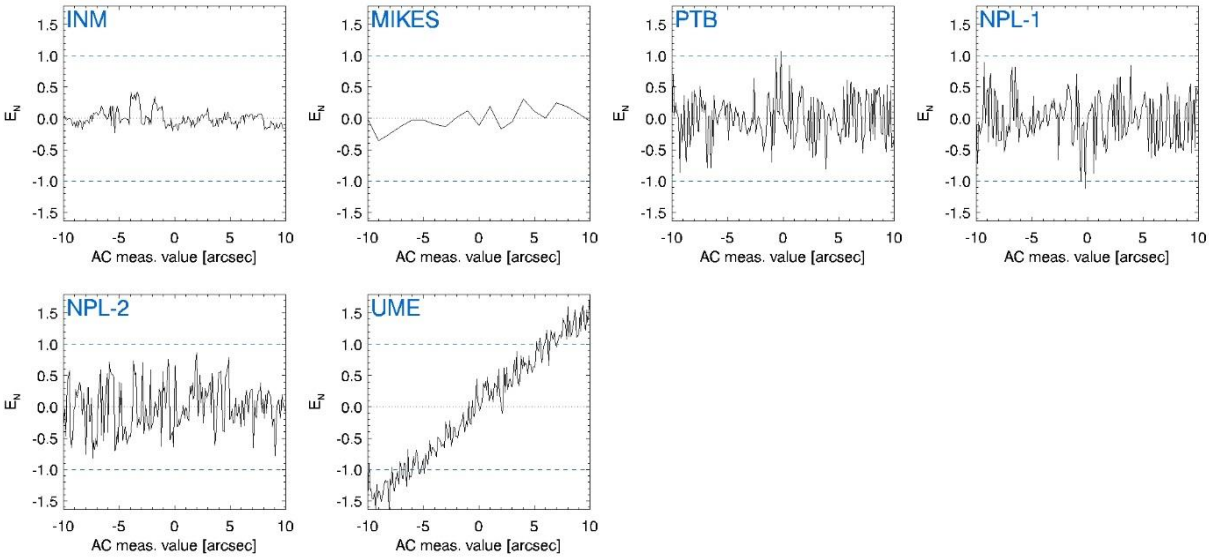

Figure 7-4. Data set S1-SR: Deviations of the participants' calibrations from the KCRV characterised by their E_{N} values.

7.4.2 Results for standard S1 – large measuring range LR

In Figures 7-5 – 7-7, data are presented for measurements performed by use of the standard S1 (before repair) over the large measuring range (LR) of ± 1000 arcsec (data set S1-LR). Detailed explanations of the graphs and the table have already been provided in Section 7.4.1. In the large measuring range, a v-shaped increase in the standard uncertainties for the KCVR values is discernible, see Figure 7-5(b). It is caused by the uncertainty contribution due to the unknown refractive index of the air, mainly due to the air pressure, see Section 5 for details.

Table 7-3 presents the data in tabular form. For no participant, multiple measures indicate significant mismatches between the deviations from the KCRV and the stated uncertainties which need explanation and warrant further investigation.

Table 7-3. Deviations of the participants' calibrations from the KCRV for data set S1-LR.

NMI	Country	Initial std. unc. α = 1000" [arcsec]	Corrected std. unc. α = 1000" [arcsec]	Std. dev. E_N	Range E_N [min., max.]	Fraction [%] $\lvert E_N \rvert > 1$
NPL-2[b]	United Kingdom	0.030	0.039	0.03	[-0.08, 0.15]	0.0
UME-2[a]	Turkey	0.030	0.033	0.06	[-0.18, 0.17]	0.0
UME-3[a]	Turkey	0.030	0.033	0.07	[-0.20, 0.13]	0.0
NPL-1[b]	United Kingdom	0.030	0.039	0.07	[-0.16, 0.17]	0.0
UME-1[a]	Turkey	0.030	0.033	0.12	[-0.30, 0.24]	0.0
PTB	Germany	0.003	0.015	0.20	[-0.42, 0.42]	0.0
MIKES	Finland	0.010	0.018	0.21	[-0.52, 0.46]	0.0
LNE	France	0.030	0.034	0.22	[-0.55, 0.42]	0.0
METAS	Switzerland	0.054	0.056	0.31	[-0.77, 0.70]	0.0
INM	Romania	0.188	0.188	0.34	[-0.70, 0.45]	0.0

a, b: Calibrations were obtained by use of different mirrors.

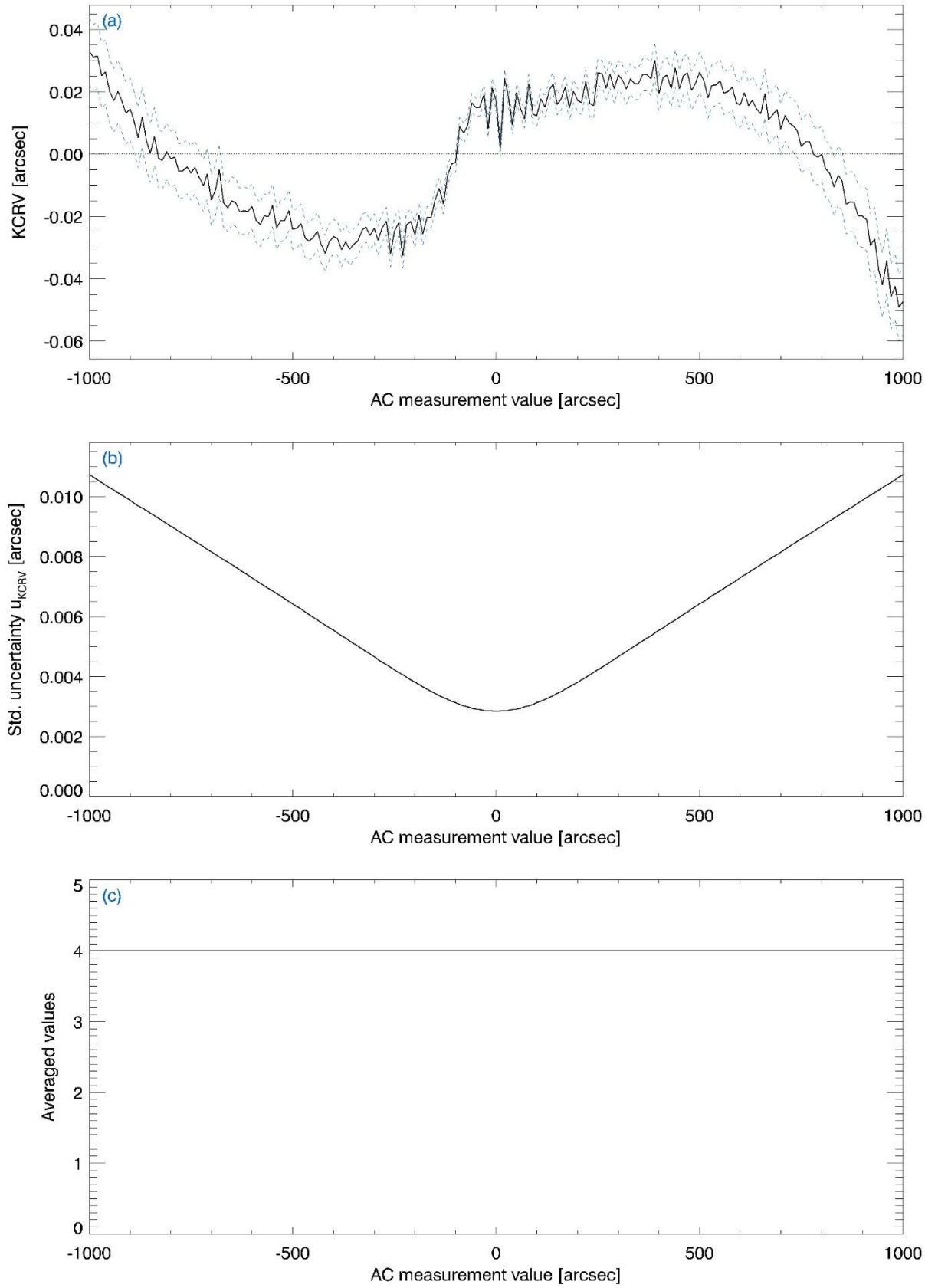

Figure 7-5. Data set S1-LR: (a) KCRV values (solid, black line) and the range (dashed, blue lines) given by the associated standard uncertainties. (b) Standard uncertainties of the KCRV values. (c) Number of participants included in KCRV values (due to the differing sampling of the participants).

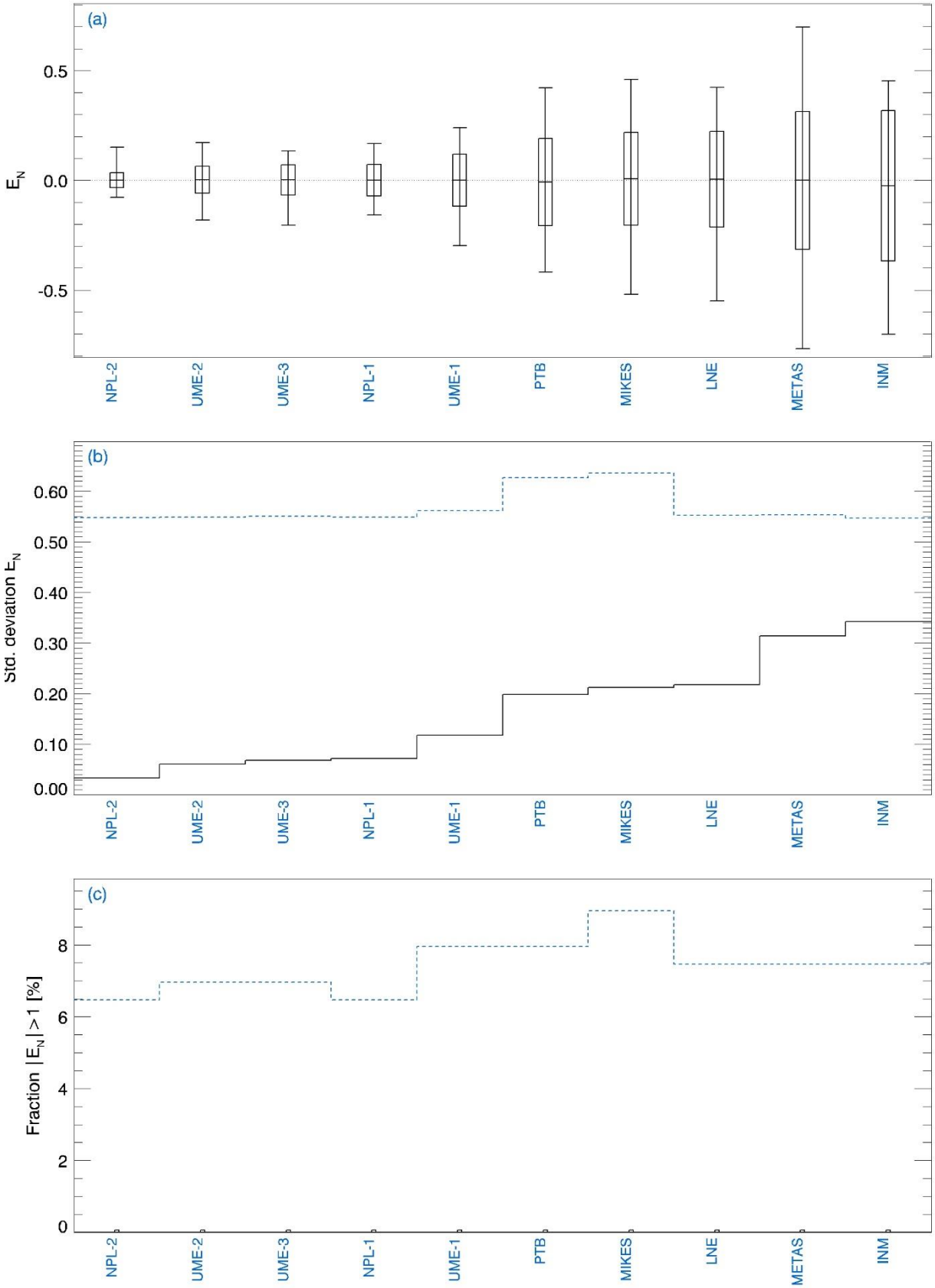

Figure 7-6. Data set S1-LR: Deviations of the participants' calibrations from the KCRV. (a) Box plots of the E_N values, see text for details. (b) Standard deviations of the E_N values (solid, black line) and MC-based upper limits associated with a 95% coverage probability (dashed, blue line). (c) Fraction of values $|E_N| > 1$ (solid, black line) and 95% upper limits (dashed, blue line).

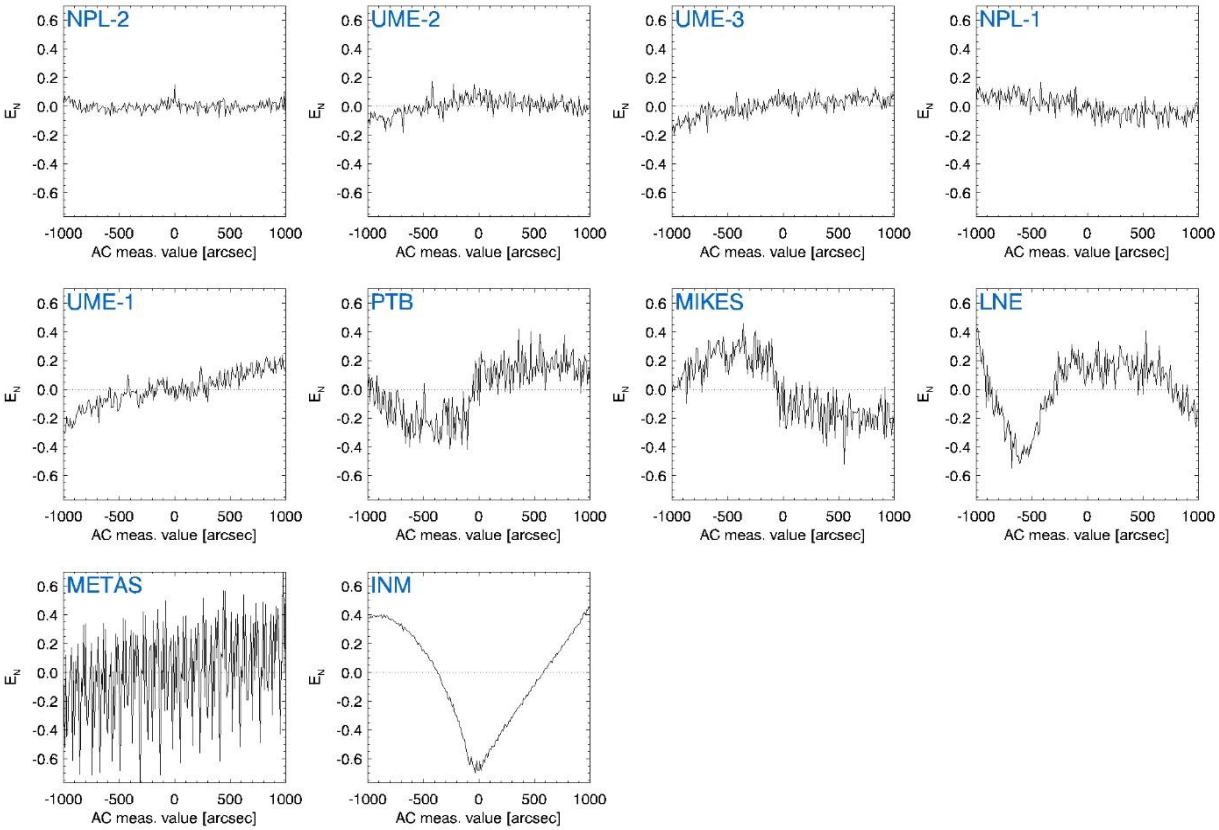

Figure 7-7. Data set S1-LR: Deviations of the participants' calibrations from the KCRV characterised by their E_{N} values.

7.4.3 Results for standard S2 – small measuring range SR

In Figures 7-8 – 7-10, data are presented for measurements performed by use of the standard S2 (after repair) over the small measuring range (SR) of ± 10 arcsec (data set S2-SR). Detailed explanations of the graphs and the table have already been provided in Section 7.4.1. As noted, in Figures 7-9(b) & 7-9(c), the limit for each measure is shown (dashed, blue line) below which 95% of the MC-simulated values for the respective measure are located. In case that a participant's value exceeds the limit, it is marked by an asterisk. An additional asterisk signifies that the participant's measurements also violate the multiple hypothesis testing according to the approach outlined in Section 6.3.6, Equation (6-17).

Table 7-4 presents the data in tabular form. For one participant, multiple measures indicate significant mismatches between the deviations from the KCRV and the stated uncertainties which need explanation and warrant further investigation. This is the case for VNIIM.

Table 7-4. Deviations of the participants' calibrations from the KCRV for data set S2-SR.

NMI	Country	Initial std. unc. α = 10″ [arcsec]	Corrected std. unc. α = 10″ [arcsec]	Std. dev. E_N	Range E_N [min., max.]	Fraction [%] $\lvert E_N \rvert > 1$
CMI-1[a]	Czech Republic	0.080	0.080	0.02	[-0.04, 0.02]	0.0
BIM	Bulgaria	0.250	0.250	0.04	[-0.10, 0.07]	0.0
VSL	Netherlands	0.040	0.040	0.10	[-0.22, 0.22]	0.0
NMI (C)	China	0.035	0.035	0.10	[-0.23, 0.28]	0.0
A-Star	Singapore	0.080	0.080	0.10	[-0.19, 0.17]	0.0
NMIA	Australia	0.055	0.055	0.11	[-0.25, 0.16]	0.0
MKEH	Hungary	0.090	0.090	0.15	[-0.33, 0.37]	0.0
CEM	Spain	0.090	0.090	0.15	[-0.36, 0.50]	0.0
INPL	Israel	0.050	0.050	0.17	[-0.31, 0.35]	0.0
NMIJ	Japan	0.005	0.005	0.20	[-0.64, 0.45]	0.0
NIMT	Thailand	0.110	0.110	0.21	[-0.33, 0.36]	0.0
DMDM	Serbia	0.100	0.100	0.21	[-0.38, 0.50]	0.0
PTB	Germany	0.003	0.003	0.23	[-0.46, 0.82]	0.0
CMI-2[a]	Czech Republic	0.010	0.010	0.24	[-0.57, 0.41]	0.0
SMU	Slovak Republic	0.025	0.025	0.27	[-0.40, 0.39]	0.0
IPQ	Portugal	0.088	0.088	0.37	[-0.75, 0.64]	0.0
GUM	Poland	0.033	0.033	0.49	[-1.37, 0.86]	5.0
VNIIM	Russia	0.004	0.004	1.36	[-2.50, 2.66]	51.7

a: Calibrations were obtained by use of different calibration set-ups.

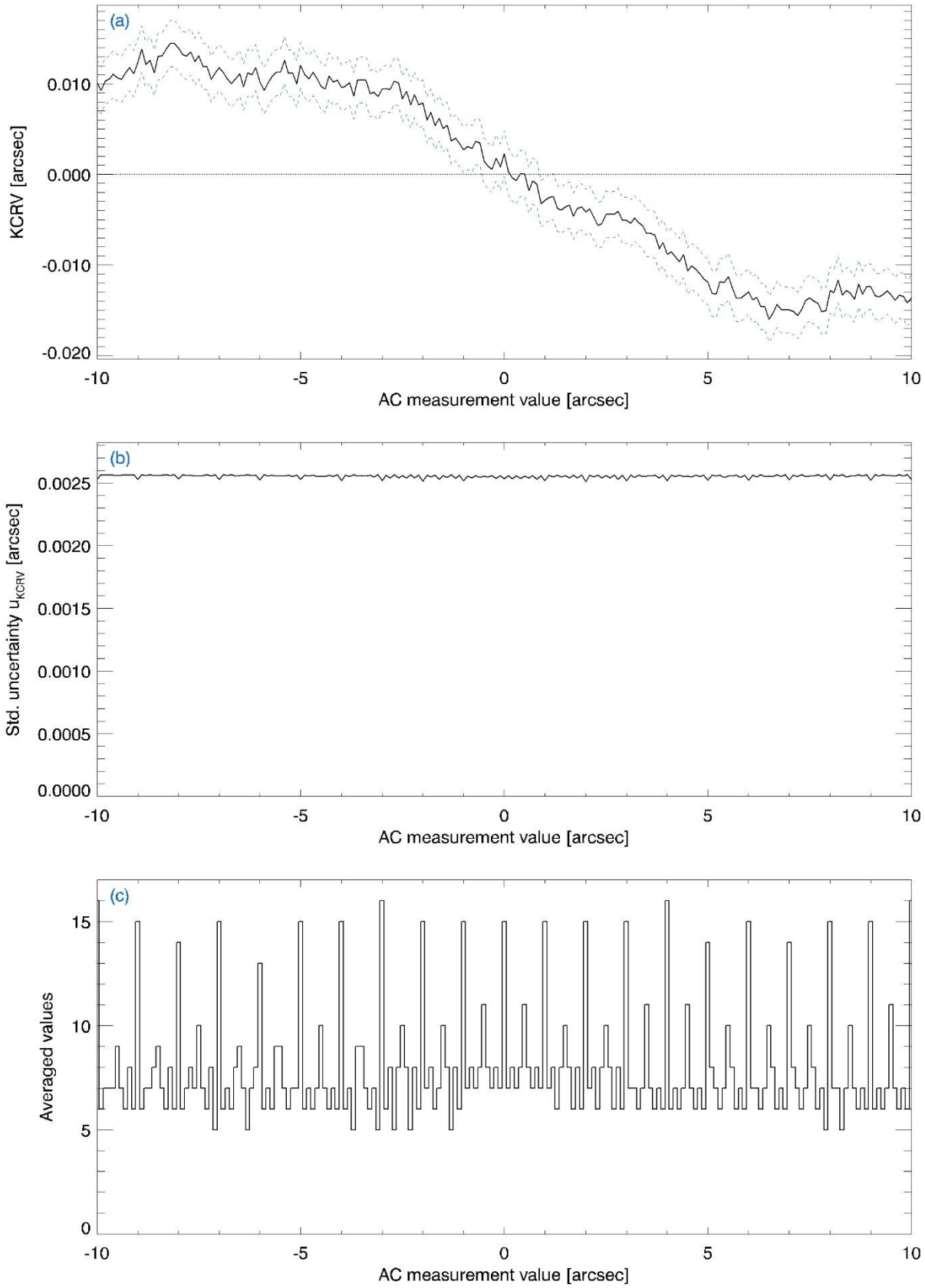

Figure 7-8. Data set S2-SR: (a) KCRV values (solid, black line) and the range (dashed, blue lines) given by the associated standard uncertainties. (b) Standard uncertainties of the KCRV values. (c) Number of participants included in KCRV values (due to the differing sampling of the participants).

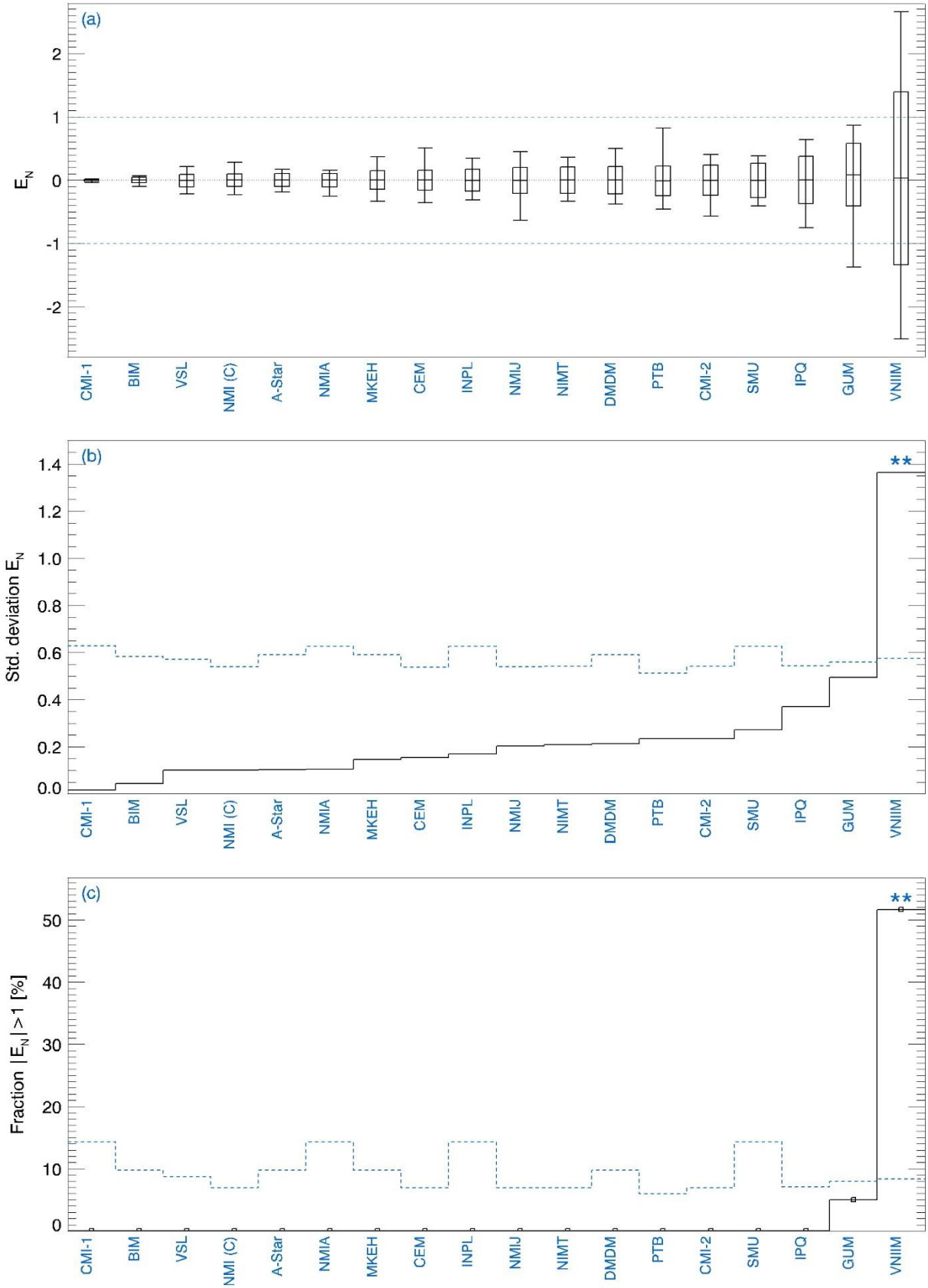

Figure 7-9. Data set S2-SR: Deviations of the participants' calibrations from the KCRV. (a) Box plots of the E_N values, see text for details. (b) Standard deviations of the E_N values (solid, black line) and MC-based upper limits associated with a 95% coverage probability (dashed, blue line). (c) Fraction of values $|E_N| > 1$ (solid, black line) and 95% upper limits (dashed, blue line).

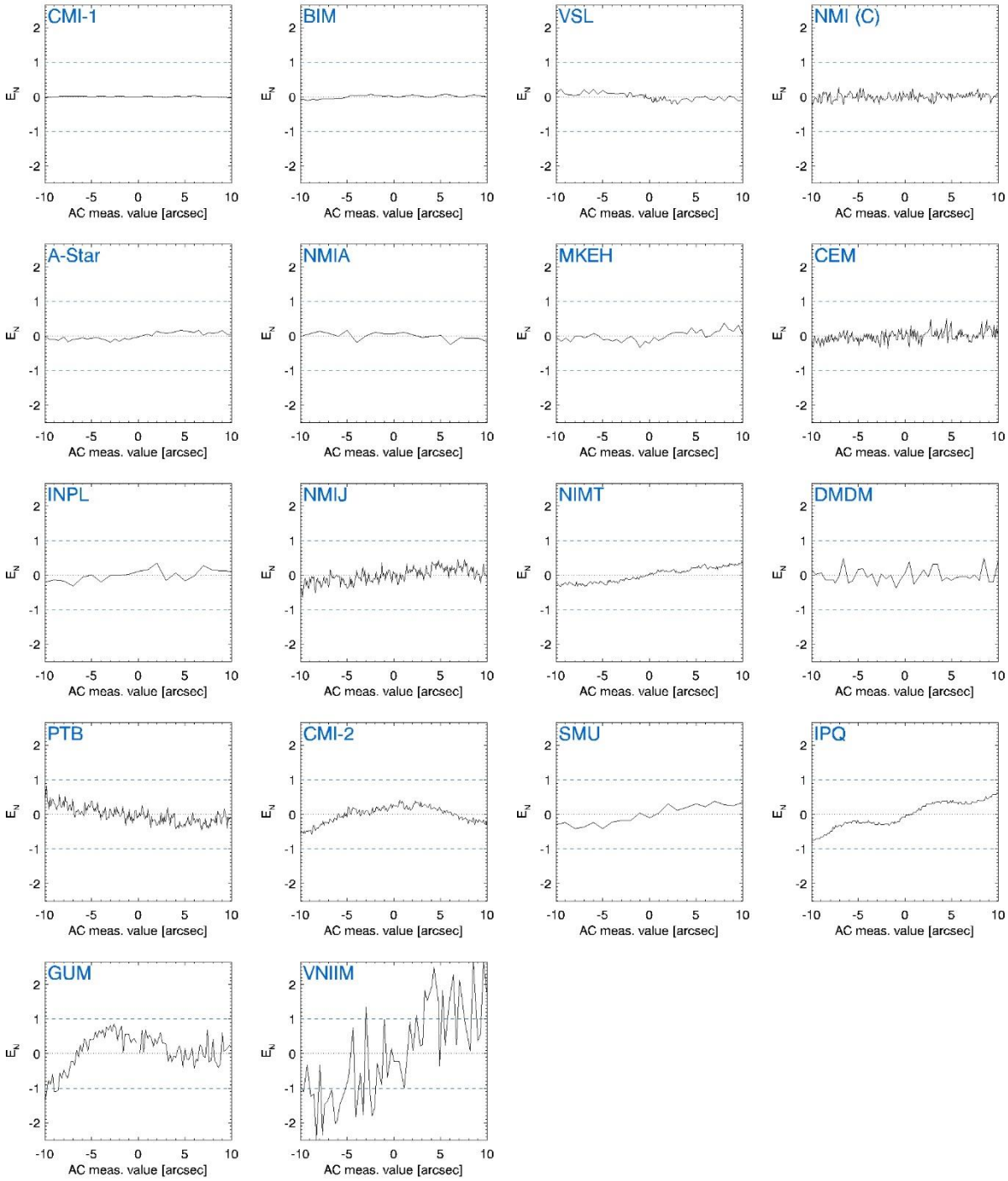

Figure 7-10. Data set S2-SR: Deviations of the participants' calibrations from the KCRV characterised by their E_{N} values.

7.4.4 Results for standard S2 – large measuring range LR

In Figures 7-11 – 7-13, data are presented for measurements performed by use of the standard S2 (after repair) over the large measuring range (LR) of ± 1000 arcsec (data set S2-LR). Detailed explanations of the graphs and the table have already been provided in Section 7.4.1.

Table 7-5 presents the data in tabular form. For three participants, multiple measures indicate significant mismatches between the deviations from the KCRV and the stated uncertainties which need explanation and warrant further investigation. This is the case for RCM-LIPI, GUM, and MKEH.

Table 7-5. Deviations of the participants' calibrations from the KCRV for data set S2-LR.

NMI	Country	Initial std. unc. α = 1000″ [arcsec]	Corrected std. unc. α = 1000″ [arcsec]	Std. dev. E_N	Range E_N [min., max.]	Fraction [%] $\lvert E_N \rvert > 1$
CMI-1[a]	Czech Republic	0.080	0.081	0.07	[-0.11, 0.14]	0.0
A-Star	Singapore	0.280	0.280	0.08	[-0.26, 0.22]	0.0
VSL	Netherlands	0.040	0.043	0.10	[-0.30, 0.18]	0.0
BIM	Bulgaria	0.250	0.251	0.10	[-0.26, 0.20]	0.0
INRIM	Italy	0.071	0.073	0.11	[-0.33, 0.21]	0.0
INPL	Israel	0.080	0.080	0.11	[-0.25, 0.24]	0.0
PTB	Germany	0.003	0.015	0.19	[-0.57, 0.72]	0.0
NIMT	Thailand	0.125	0.126	0.20	[-0.63, 0.40]	0.0
NMIJ	Japan	0.005	0.015	0.24	[-0.46, 0.60]	0.0
NPL (I)	India	0.218	0.219	0.26	[-0.69, 0.47]	0.0
CMI-2[a]	Czech Republic	0.022	0.026	0.30	[-0.69, 0.56]	0.0
NMI (C)	China	0.035	0.038	0.32	[-0.59, 0.65]	0.0
VNIIM	Russia	0.028	0.032	0.37	[-1.29, 0.59]	2.4
SMU	Slovak Republic	0.025	0.035	0.41	[-0.94, 0.88]	0.0
DMDM	Serbia	0.100	0.100	0.42	[-0.95, 0.99]	0.0
IPQ	Portugal	0.088	0.090	0.44	[-1.00, 0.81]	0.0
CEM	Spain	0.086	0.088	0.44	[-0.80, 0.97]	0.0
NMIA	Australia	0.055	0.057	0.49	[-1.05, 0.88]	4.8
RCM-LIPI	Indonesia	0.110	0.111	0.69	[-1.77, 2.01]	15.4
GUM	Poland	0.088	0.089	0.73	[-2.62, 1.82]	15.4
MKEH	Hungary	0.090	0.091	1.04	[-2.18, 1.52]	29.8

a: Calibrations were obtained by use of different calibration set-ups.

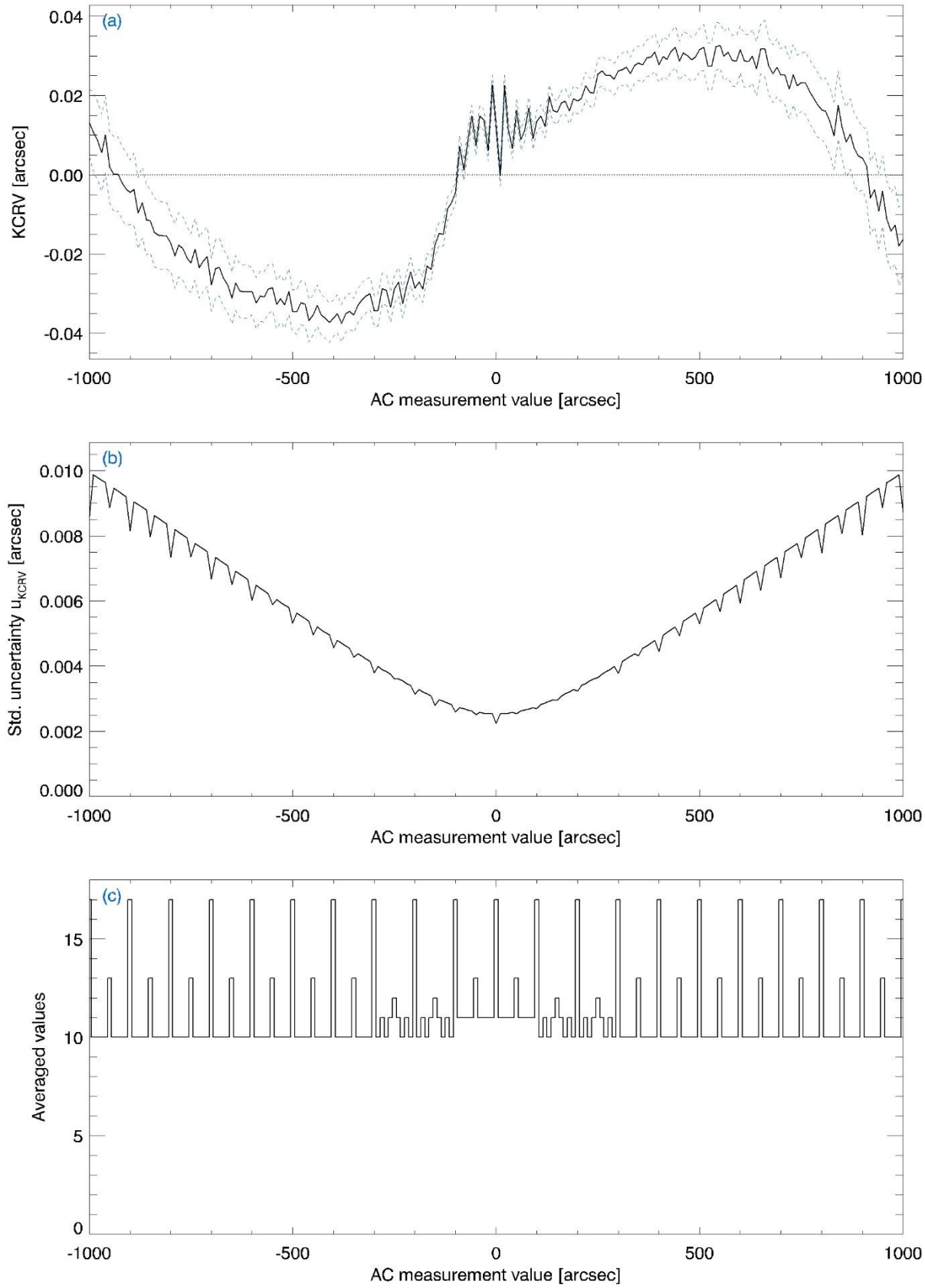

Figure 7-11. Data set S2-LR: (a) KCRV values (solid, black line) and the range (dashed, blue lines) given by the associated standard uncertainties. (b) Standard uncertainties of the KCRV values. (c) Number of participants included in KCRV values (due to the differing sampling of the participants).

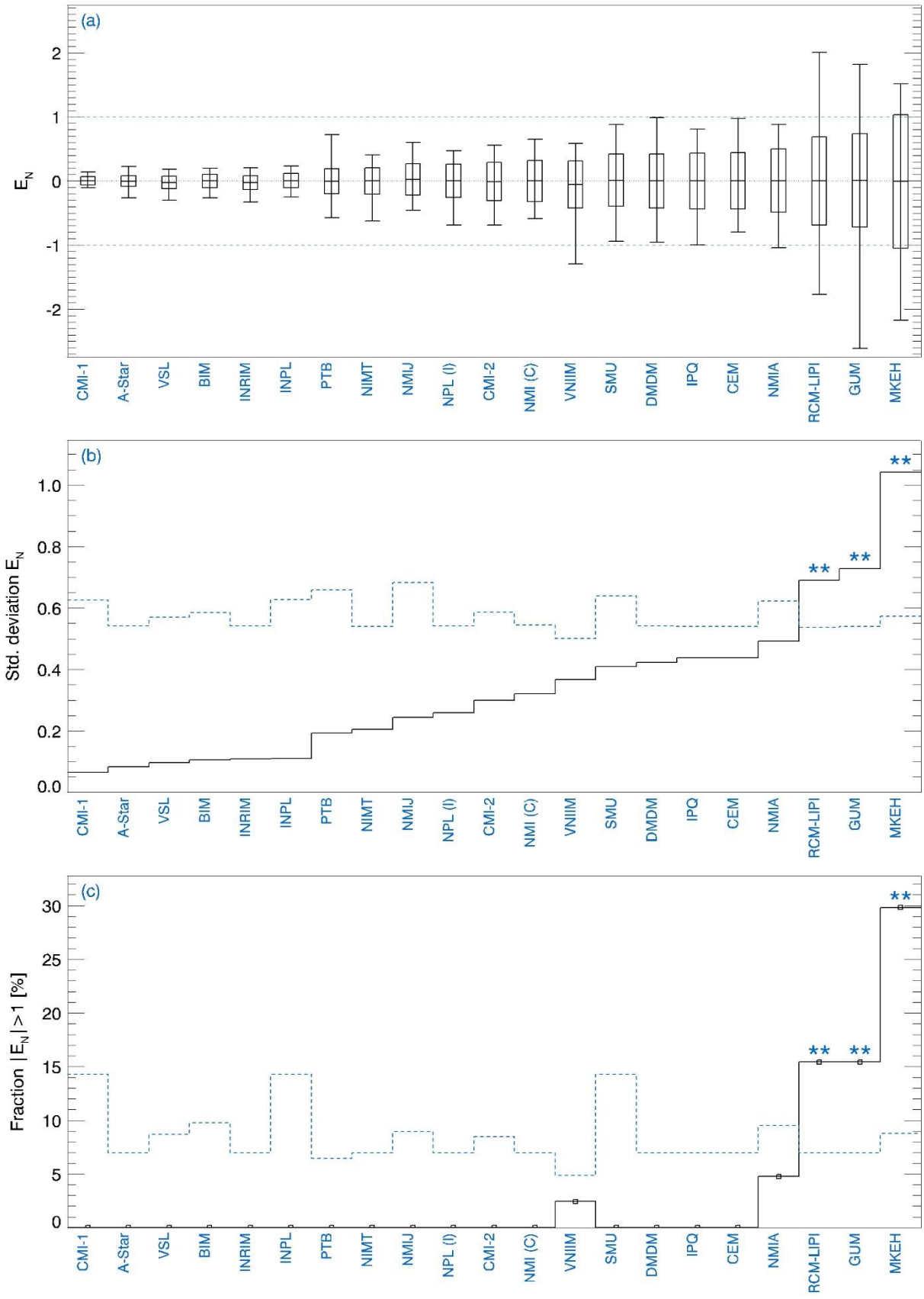

Figure 7-12. Data set S2-LR: Deviations of the participants' calibrations from the KCRV. (a) Box plots of the E_N values, see text for details. (b) Standard deviations of the E_N values (solid, black line) and MC-based upper limits associated with a 95% coverage probability (dashed, blue line). (c) Fraction of values $|E_N| > 1$ (solid, black line) and 95% upper limits (dashed, blue line).

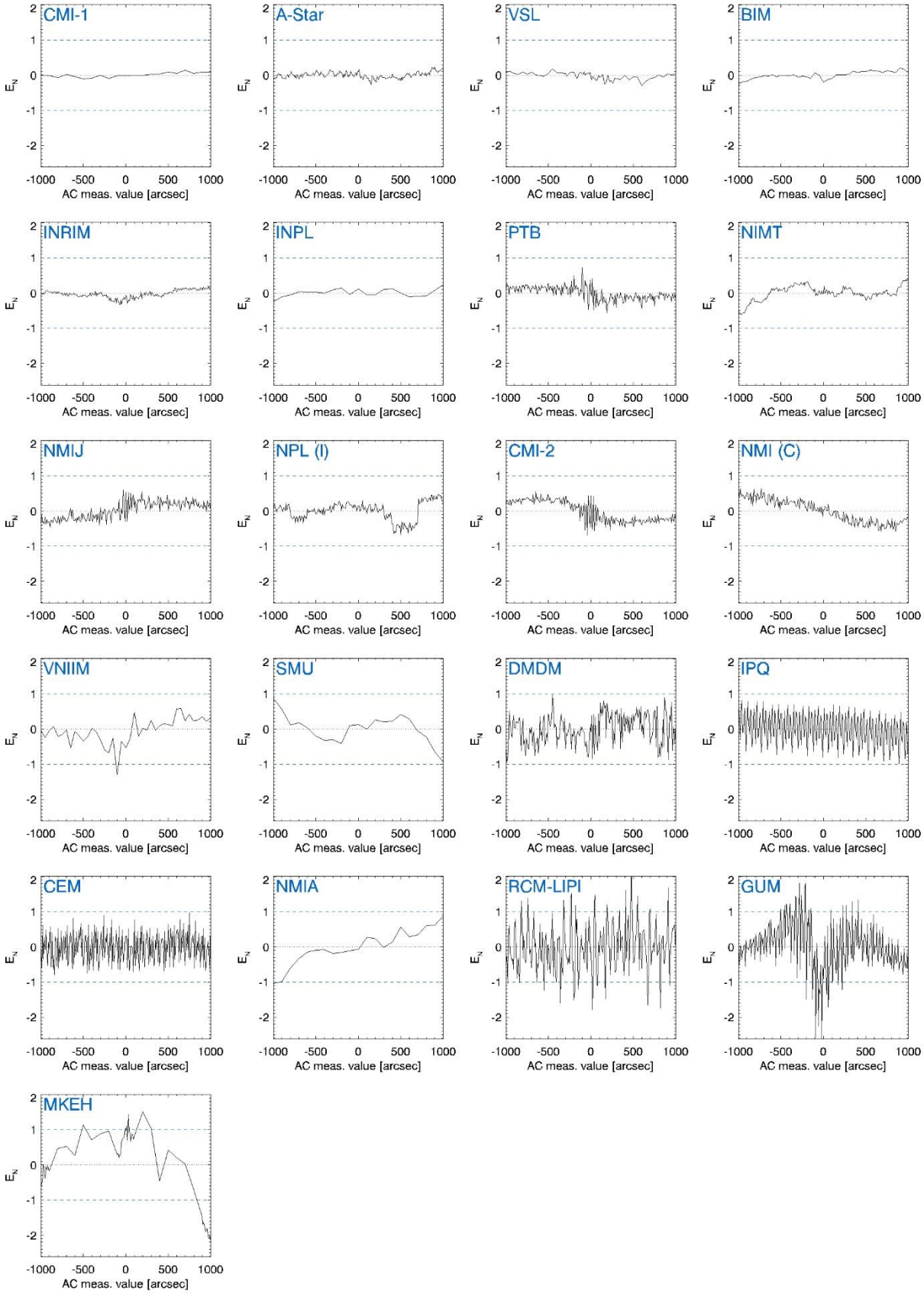

Figure 7-13. Data set S2-LR: Deviations of the participants' calibrations from the KCRV characterised by their E_{N} values.

8 Participant's comments

Comment METAS 13.08.2010

The calibration of the autocollimator in the range of ±1000" is done in direct comparison with the METAS angle comparator. The angular encoder Heidenhain RON 905 of this comparator exhibits an interpolation error, which can only be partly corrected. The residual interpolation error became apparently larger in the last year and gives rise to peak-valley deviations of 0.15". This error could not be removed from the measurement data and determines strongly the measurement uncertainty.

The calibration of the autocollimator in the range of ±10" was intended to be performed using a DPT-activated Zerodur sinebar with a range of ± 7.5 µm (corresponding to ±7.5"), and then stitching the overlapping results to ±10". The measurements with this equipment have shown so far unexplained non-linearities and hysteresis. We haven't used this equipment since several years. We have decided not to submit these results within the comparison, because they are strongly compromised by unexplained deviations and are thus not significant. We shall not deliver any customer services in this field, until we have solved the problem, or we might withdraw our CMC.

Comment VSL 30.08.2011

We seem to have found the cause of our erroneous results. The mechanical construction we use to generate the angle appears to behave in an unexpected way at its pivoting points. Since our measurement method does not correct for the resulting translational movements at the pivoting points, the calculated angles were slightly wrong. We will take action to improve the setup and modify the measurement method in the coming months so we will be prepared in time for the second calibration you have offered us.

Comment INM 01.06.2011

After data verification review of measurement uncertainty:

Combined standard measurement uncertainty

u(d) = ((0.049^2+(0.00012*a)^2)^(1/2) = 0.13 arcsec (for a=1000 sec.)

rev. 2011:

Combined standard measurement uncertainty

u(d) = ((0.14455^2+(0.00012*a)^2)^(1/2) = 0.19 arcsec (for a=1000 sec.)

Comment SMU 15.06.2012

Observed of a damage at the measuring device (loose store roller), after the repair of the small angle generator, re-calibration of the AC.

Comment IPQ 06.02.2015

After the re-evaluation of the data. It was made an update of the measurement uncertainty.

Revision of uncertainty budget: (u = 0,088" instead of u = 0,06")

Comment EIM 12.06.2015

We would like to inform you that we are going to withdrawn from EURAMET.L-K3.2009 Key Comparison. Sorry for any inconvenience we caused you.

Comment SMD 12.06.2015

The colleague who made the measurements has left SMD shortly after doing so. It shows to be too difficult to reconstruct reliable measurement results from the data that he has left. there is only reliable data for one measurement run in each direction, which is insufficient for repeatability evaluation. Furthermore there are some strange deviations at some points, totally different from the deviations at the surrounding points. So we like to withdraw from this comparison.

Comment NPL India 15.07.2015

The results were not corrected against the errors of NPL, India auto-collimator. These errors are the NPL India auto-collimator calibration certificate results (Traceable to PTB); instead the maximum value of error over the entire range of NPL-India auto-collimator is considered for calculating an uncertainty component of Bias.

Revision of uncertainty budget: (u = 0,218" instead of u = 0,015")

Comment DMDM 15.07.2015

I checked the measuring data and I found a few mistakes. We did not correctly type and rounded values in excel during calculations of average values/subtracting zero values from measuring point values. If it would be possible, I ask you, please, to correct our previous values to the new corrected values, as follows.

At -450° meas. point result is +0,17 arcsec instead of +0,21 arcsec

At -620° meas. point result is -0,16 arcsec instead of -0,20 arcsec

At +110° meas. point result is +0,17 arcsec instead of +0,20 arcsec

At +190° meas. point result is +0,17 arcsec instead of +0,22 arcsec

At +910° meas. point result is -0,17 arcsec instead of -0,20 arcsec

Comment NIMA 27.10.2015

Thank you for the preliminary data. I checked NMIA's results and they are all correct (unfortunately!). I suspect the cause of our poor agreement maybe an error associated with the base length of our small angle generator. In use we have to attach an extension rod to a digital indicator to measure vertical displacement of the arm. We always assumed that the extension rod was coaxial with the indicator and I now suspect that this is not the case, resulting in a slightly altered baselength. In future we will make modifications to remove this shortcoming. I guess that's one of the reasons why intercomparisons are so useful!.

Comment GUM 04.03.2016

Decision GUM: Deleting these values (measurement with GUM mirror)

…But we have decided to withdraw the results obtained from GUM mirror. This mirror is the old one with rather poor metrological characteristics. Now we don't use it at all.

Comment INRIM 03.03.2016

Decision INRIM: Deleting these values (from measurement in LOOP 1)

We have presented results for the +/- 1000 calibration both in loop 1 and in loop 2. The reason why we wanted to participate also to loop 2 was because we were not satisfied about our calibration set-up and, indeed, we brought up several improvements before the measurement in loop 2. For this reason, also considering that the procedure used in loop 1 is not used anymore, if you agree, we would like to cancel the data of loop 1 and confirm the data of loop 2.

Comment MKÈH 09.11.2016

…We would also like to ask you to involve some comments in the final protocol. We had a comment at that time, that we used not the PTB reflector but our own that also could cause some errors. The En values show good results for the 10" range, we had problem in the 1000" range. We have no CMC and we would not have it in the near future.

Comment RCM-LIPI 15.11.2016

About our data, that's all we got during comparison. By seeing the result, we saw that our data were not good. After comparison and draft A result, we investigated our system and our standard, we thought something is not right regarding our standard. Now we are sending our standard to Japan to be repair.

Comment UME 15.06.2017 (T. Yandayan)

UME gives comments on the linear drift of their results for the measurements taken at the short range (±10") with a standard uncertainty of 0.005". These comments are also important to evaluate the performance of autocollimators for high precision applications e.g. nanoradian angle metrology [UME-1].

UME performed the measurements using two different reference system for two different ranges with two different uncertainties which differs six times in the ratio as given below.

Code for the loop	Range	Standard uncertainty	Reference measurement system
S1-SR	±10"	0.005"	High Precision Small Angle Generator (HPSAG) made by UME used with sampling points of 0.1".
S1-LR	±1008"	0.030	UME angle comparator (Rotary Table) custom made by KUNZ used with sampling points of 7.2".

UME results for S1-LR (±1008") with uncertainty (0.03") has very good agreement with the KCRV.

UME results in short range, S1-SR (±10") with uncertainty (0.005") suffered from a linear slope due to large initial angle offset not taken into consideration. Therefore, results of UME for the range larger than ±5" produced E_N values greater than 1 as seen in Fig. UME-1. This was investigated and explained below.

Reason for linear deviation of UME results in (S1-SR) with the range (±10") is illustrated in Fig. UME-2. During the set-up of the reference system (HPSAG), this initial angle was not properly adjusted to be zero or not corrected using the given formula for the results. This caused the deviation of the results with a linear slope for the measured small range (±10"). In Fig. UME-3, the results of UME with HPSAG in S1-SR (±10") are illustrated with KCRV, before (blue) and after slope correction (red).

To do better analysis, we have also added our results of Rotary Table taken at the measurements points of (-14.4, -7.2, 0, 7.2, 14.4)" for the range of S1-LR (±1008"). They are illustrated in Fig. UME-3 as UME-1, UME-2 and UME-3 results (taken from section 7.4.2 Results of standard S1 - large measuring range LR in the report). When the results taken by the HPSAG are corrected due to this initial angle (*i.e. when the equation shown for α in Fig. UME-2 is used*), we get results (UME_SlopeCorrect) that are in good agreement with the KCRV and also with the results taken by our Rotary table (Fig. UME-3). It should also be noted that Rotary table results of UME taken with different mirrors (UME-1, -2,-3) have good agreement with the KCRV for the short range S1-SR (±10") as well (see Fig. UME-3). The E_N values of UME given in Fig. UME-1 (from Fig. 7-4 of the results in the report) also support this argument very well. The variation of E_N values for multiple sampling points (e.g. successive ones), i.e. bandwidth - apart from the linear slope is very small. This means that if the results were corrected using the α equation in Fig. UME-2 for the slope, or if the initial angle was better adjusted as near as possible to

be zero, the results would be in very good agreement with the KCRV (see Fig. UME-3). This can also be observed in Fig. UME-1 with the red bandwidth lines.

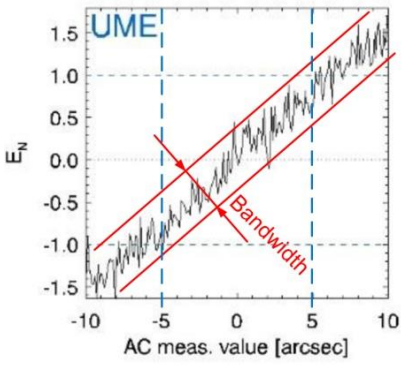

Fig. UME-1. E_N values of UME in data set of S1-SR (from Fig. 7-4 of the report).

Sine arm misaligned by α_0 ,

(it has initial angle at starting position to datum)

$$\alpha_0 = \arcsin\left(\frac{h_0}{L}\right)$$

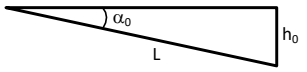

In this case, it measures angle α

$$\boldsymbol{\alpha = \arcsin\left[\sin(\alpha_0) + \frac{h}{L}\right] - \alpha_0}$$

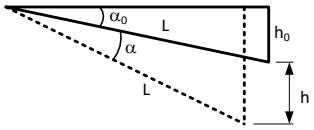

Fig. UME-2. Explanations for cause of the slope deviation in the results of UME for S1-SR.

According to slope corrected results of UME in Fig. UME-3, we can conclude that the used autocollimator is an excellent transfer standard for investigation of participants capabilities even for the very small angle steps (e.g. 0.1"). Calibration of Autocollimator with different devices agrees in amplitude and also in lateral positions in the order of a few milliarcsec. After slope correction, difference between UME and KCRV results is 0.002" (rms). It should also be noted that the HPSAG used for UME results has a range of ±8". Therefore, the results of UME shown in Fig. UME-3 were obtained by stitching 3 sets of results obtained at ranges (-10 to 0)", (±8"), and (0 to 10)". Reproducibility for measurements obtained using different scales of the HPSAG (for 3 sets) is considerably good that such agreement with KCRV results exist.

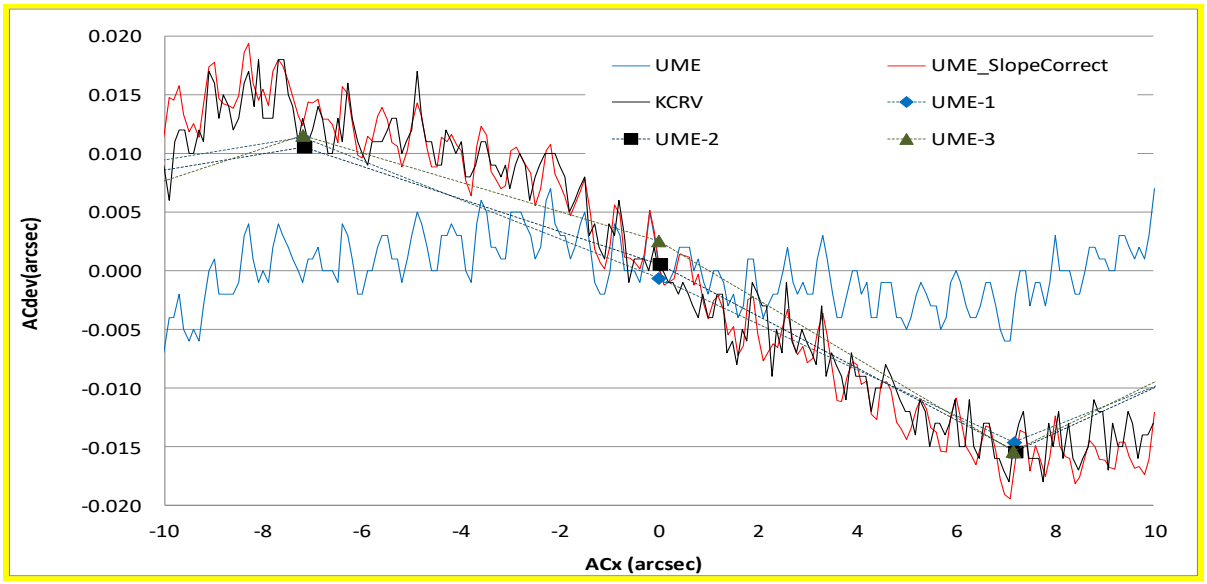

Fig. UME-3. UME results in (S1-SR) with the KCRV, before (blue) and after slope correction (red) including UME Rotary Table results taken at the sampling points (-14.4, -7.2, 0, 7.2, 14.4)" for the range of S1-LR (±1008") as UME-1, UME-2 and UME-3.

It is indeed unfortunate that initial angle problem (described in Fig. UME-2) was missed and such agreement would not be proved officially. Since UME has no CMC entry with such small uncertainty with this system, there is no need to perform any corrective action. But UME has already developed new type small angle generator in SIB58 Angle project [UME-2]. The device can calibrate larger ranges than the current one (with better performance) up to a few thousand arc seconds as well as in very small steps (e.g. 0.0005", see UME-2). This device will participate another comparison later.

Note: Considering the performance of the UME's rotary table for the short range S1-SR (±10") and also for the long range S1-LR (±1008"), one can conclude that standard uncertainty of 0.03" was over estimated. The reason behind this was due to unknowns in the errors of the rotary table on that time (2010). The multiple sampling step was chosen as 7.2" (basic resolution) to reduce the interpolation error and also the uncertainty was increased. The system has recently been modernized with better interpolators and fully investigated using error separation methods (shearing technique) [3]. UME also plans to attend another comparisons with lower uncertainty than 0.03" using the new interpolators at any multiple sampling points.

References

[UME-1] Tanfer Yandayan and Ralf Geckeler, "Demands for nanoradian angle metrology and performance requirements on autocollimators", euspen's 17th International Conference & Exhibition, Hannover, DE, May 2017. (www.euspen.eu).

[UME-2] Tanfer Yandayan " A portable Large Range Small Angle Generator (LRSAG) for precise calibration of autocollimators ", euspen's 17th International Conference & Exhibition, Hannover, DE, May 2017. (www.euspen.eu).

[UME-3] Tanfer Yandayan, Ralf D. Geckeler, Andreas Just, Michael Krause, S. Asli Akgoz, Murat Aksulu, Bernd Grubert and Tsukasa Watanabe" Investigations of interpolation errors of angle encoders for high precision angle metrology ", submitted to MacroScale 2017, Recent developments in traceable dimensional measurements, Otaniemi, Espoo, Finland October 17th to 19th, 2017.

Comment CMI 10.10.2017

For calibration we used autocollimator MW Elcomat 3000 with traceability to PTB and uncertainty U = 0.008 arcsec.